Chem Soc Rev

RSC Publishing

REVIEW ARTICLE

View Article Online
View Journal

Manipulating biological agents and cells in micro-scale volumes for applications in medicine

Cite this: DOI: 10.1039/c3cs60042d

Savas Tasoglu,[a] Umut Atakan Gurkan,†[a] ShuQi Wang[a] and Utkan Demirci*[ab]

Recent technological advances provide new tools to manipulate cells and biological agents in micro/nano-liter volumes. With precise control over small volumes, the cell microenvironment and other biological agents can be bioengineered; interactions between cells and external stimuli can be monitored; and the fundamental mechanisms such as cancer metastasis and stem cell differentiation can be elucidated. Technological advances based on the principles of electrical, magnetic, chemical, optical, acoustic, and mechanical forces lead to novel applications in point-of-care diagnostics, regenerative medicine, *in vitro* drug testing, cryopreservation, and cell isolation/purification. In this review, we first focus on the underlying mechanisms of emerging examples for cell manipulation in small volumes targeting applications such as tissue engineering. Then, we illustrate how these mechanisms impact the aforementioned biomedical applications, discuss the associated challenges, and provide perspectives for further development.

Received 3rd February 2013

DOI: 10.1039/c3cs60042d

www.rsc.org/csr

[a] *Bio-Acoustic-MEMS in Medicine (BAMM) Laboratory, Division of Biomedical Engineering and Division of Infectious Diseases, Department of Medicine, Brigham and Women's Hospital, Harvard Medical School, Boston, MA, USA. E-mail: udemirci@rics.bwh.harvard.edu*

[b] *Harvard-MIT Health Sciences and Technology, Cambridge, MA, USA*

† Present address: Case Biomanufacturing and Microfabrication Laboratory, Mechanical and Aerospace Engineering, Case Western Reserve University, Advanced Platform Technology Center, Louis Stokes Cleveland Veterans Affairs Medical Center, Cleveland, OH, USA.

1. Introduction

This review focuses on emerging micro- and nano-scale bioengineering and biomedical microfluidic technology platforms at the convergence of engineering, biology and materials science with an emphasis on broad biotechnology applications in medicine. Strategies have been sought to manipulate cells spatially to develop a better understanding of living systems.

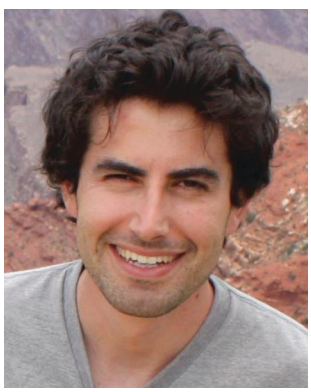

Savas Tasoglu

Dr Tasoglu received his PhD from UC Berkeley. His current research interests at Harvard are magnetics, neurotechnologies, microfluidics, cell and tissue mechanics, regenerative medicine, microbicides, cryopreservation, and cell-based diagnostics for point-of-care. Dr Tasoglu's achievements in research and teaching have been recognized with numerous fellowships and awards including Chang-Lin Tien Fellowship in Mechanical Engineering, Allen D. Wilson Memorial Scholarship, and UC Berkeley Institute Fellowship for Preparing Future Faculty. Dr Tasoglu's three articles with first authorship featured the cover of prestigious journals such as Advanced Materials, Trends in Biotechnology, and Physics of Fluids.

Umut Atakan Gurkan

Dr Gurkan is leading the CASE Biomanufacturing and Microfabrication Laboratory in Mechanical and Aerospace Engineering at Case Western Reserve University. Dr Gurkan's research interests include micro/nano-engineered biological systems with applications in medicine. Dr Gurkan's collaborative clinical research and teaching have been recognized with various prestigious awards, including the IEEE-Engineering in Medicine and Biology Society Wyss Award for Translational Research and the Partners in Excellence Award for Outstanding Community Contributions. Dr Gurkan's research has been highlighted by international and national news agencies, newspapers, and scientific publishers, including MIT News, Science Daily, Wired News, Reuters, Hurriyet News, Lab Chip, and Nature Photonics.

A broad range of technologies driven by numerous mechanisms such as fluid mechanics,[1–3] chemical affinity,[4] magnetic,[5–8] electrical,[9–11] optical,[12–15] and acoustic fields[16,17] have been presented to manipulate cells and provide potential solutions to diseases. For instance, achieving high cell density and structural complexity is of great importance for engineering artificial tissues. With broad applications of hydrogels in regenerative medicine and biomedical research,[18] manipulating cell-encapsulating hydrogels *via* non-invasive external fields has emerged as a method to construct tissue models through a bottom-up engineering approach.[19] Bioprinting different cell types is another approach to create functional tissue constructs.[20,21] The ability to encapsulate and pattern single cells at physiologically relevant cell densities would allow engineering of complex tissue structures *in vitro*.[18,22] Creation of *in vitro* three-dimensional (3-D) functional tissue constructs mimicking the role, micro-architecture, and functional properties of native biological systems and human tissues could potentially reduce pre-clinical testing on animals.[19,23,24] Cost-effectiveness of gathering clinically relevant information is significantly improved through *in vitro* multivariate testing systems (*e.g.*, cell microarrays for drug screening) due to reduced reagent consumption and increased mass exchange rates between cells and their microenvironment.[23] With high-density microwells on a chip, isolation of single cells is achievable, which can be explored to elucidate the underlying mechanisms of cancer pathogenesis and metastasis, as well as to screen drug candidates at high throughput.[23]

Approaches for manipulating cells in micro/nano-scale volumes have been widely explored to improve point-of-care (POC) testing. Isolation of cells from whole blood (*e.g.*, circulating tumor cells (CTCs) for cancer research,[25] cluster of differentiation 4 positive ($CD4^+$) T-lymphocytes for human immunodeficiency virus (HIV) monitoring[26–28]) has been demonstrated using microfluidic systems *via* immuno-capture by antibodies specific to cell surface proteins.[26,28–30] Because of their versatility and affordability, these devices can be used at primary care settings to facilitate clinical decisions. On the other hand, selective capture and on-demand release of stem cells in microfluidic channels provide an attractive alternative to enrich rare cells from complex biological samples, thus creating the possibility for downstream proteomic and genomic analyses.[29,30]

Here, we present state-of-the-art technologies employed to manipulate cells at the micro-scale level for applications in medicine. This review aims to provide a comprehensive overview with a broad perspective in physics, biology, engineering and medicine by highlighting the most significant approaches to date in cell manipulation for widespread applications. We provide examples focusing on clinical applications that were enabled by these technologies from a broad range of fields including diagnostics, regenerative medicine, reproductive medicine, and biopreservation. Although these fields seem to be apart from each other, we underline how they have been impacted by these emerging micro/nano-scale technologies sharing the same core competencies enabled by our evolving technological ability to command cells and their microenvironment in micro/nano-scale volumes.

2. Theories for modelling cell manipulation

There are several methods based on magnetic, optical, electrical, and mechanical principles to manipulate cells[31] (Table 1). For instance, magnetic particles can be selectively attached to cells for cell separation or purification in microfluidic devices. There is a growing interest in optical tweezers for parallel, non-contact, and contamination-free manipulation of cells.[32,33] Manipulation of target cells can also be achieved by micro-fabricated structures such as microfilters,[34] microwells,[35] microgrippers,[36] dam structures,[37] and sandbag structures.[38] Electrical forces can be employed through electrophoresis and dielectrophoresis to manipulate cells. Dielectrophoretic forces arise from polarizability of cells, while electrophoresis arises from the interaction of cell charges and an electric field.[39,40] Here, we describe underlying mechanisms for a set of emerging techniques[41] where cell-encapsulating femto-to-nano-liter hydrogels are assembled and/or patterned into complex geometries for applications including tissue engineering.[8,19,42]

ShuQi Wang

Dr ShuQi Wang obtained his medical degree from Bengbu Medical College, China, in 2000. He further pursued his master's degree in Molecular Biology and Immunology at the Institute of Dermatology, Peking Union Medical College, Chinese Academy of Medical Sciences. In 2009, he received his PhD from the University of Cambridge, UK, focusing on rapid nucleic acid amplification technologies for HIV viral load monitoring in resource-limited settings. Presently, he is working on the development of rapid immunoassays for point-of-care diagnostics using microfluidic approaches.

Utkan Demirci

Utkan Demirci, PhD, is an Assistant Professor of Medicine and Health Sciences and Technology at Harvard University Medical School and Brigham and Women's Hospital. Dr Demirci creates nano- and micro-scale technologies providing solutions for real world problems in medicine. Dr Demirci is an internationally renowned scientist and his work has been recognized with numerous national and international awards, and highlighted in Wired Magazine, Science Daily, Reuters Healthnews, Nature Photonics, MIT Technology Review, AIP News, BioTechniques, and Biophotonics.

Table 1 Principles, advantages, and disadvantages of main technologies for cell manipulation in micro-scale volumes for applications in medicine

Applications	Principles	Advantages	Limitations
Diagnostic applications and applications in isolation, purification, and enrichment of cells	*Magnetic*:[230–232] Magnetic field gradients can be employed to capture the super paramagnetic beads (10–100 nm in diameter), and cells that are selectively attached to beads.	High specificity, high efficiency, non-contact, clean, versatile, and non-invasive.	Difficulty in separating captured cells from magnetic beads when needed.
	Electrical:[39] Dielectrophoresis (DEP) is the motion imparted on uncharged particles due to polarization when subjected to a non-uniform electric field. DEP is the electronic analog of optical tweezers.	High efficiency, high selectivity, parallel manipulation.	Low survival rate of cells, complex instrumentation.
	Chemical:[26,28–30,130] Antibody immobilization onto microfluidic channels.	High selectivity and high capture efficiency.	Chemical waste disposal, specific antibody development, lengthy procedure for antibody immobilization.
	Mechanical:[34–38] Separation of target cells can be achieved by microfabricated structures. Advantages and disadvantages are separately written in the next columns for: (1) size-dependent filter-based microfluidic devices; (2) microgrippers; (3) dam and sandbag structures.	(1) High labeling efficiency, short detection time, high reproducibility based on simple and robust experimental procedures, high detection sensitivity at cell level; (2) manipulation of single cells with minimal damage; (3) relatively easier fabrication, and can efficiently immobilize cells with minimal stress.	(1) Poor selectivity; (2) Complex fabrication procedures, poor selectivity; (3) Poor selectivity.
	Optical:[32,33] Biological molecules can be tethered to dielectric spheres, which can be captured at the focal point of an electric field gradient.	High-resolution, non-contact, contamination-free.	Limited manipulation area, complex optical setup, complex operation, and expensive instrumentation.
Applications in tissue engineering and regenerative medicine	*Magnetic assembly*:[7,8] Magnetic field gradients can be employed to actuate magnetic nano-particle (MNP) and/or free/stable radical-encapsulating hydrogels.	Non-contact, contamination-free, high throughput, low adverse effects on cells, high spatial resolution.	Although there are FDA approved magnetic particles and their release from micro-scale hydrogels are proven,[233] release from large assembled tissue constructs has to be proven.
	Acoustic assembly:[16] Acoustic fields can be used to agitate the liquid surface where cell-encapsulating hydrogels assemble.	Non-contact, contamination-free, high throughput, low adverse effects on cells, low complexity.	Low spatial resolution.
	Surface tension driven assembly:[4] Tendency of multiphase liquid–liquid systems to minimize the surface area and to reach a lower energy configuration is used.	Low complexity.	Low spatial resolution, low throughput.
	Microfluidic assembly:[234–236] Microfabricated fluidic channels can be used as rails to transport hydrogel blocks.	High spatial resolution, low adverse effects on cells.	Complex fabrication, low throughput.
	Ratchet assembly:[237] Unidirectional surfaces offer to assemble cell-encapsulating microgels *via* sequential assembly processes.	Low adverse effects on cells.	Complex fabrication procedures.
	Bioprinting: Several bioprinting methods based on acoustic,[17,79] inkjet,[80,81] valve-based,[47,78,82,83] and laser printing[13,22,84] technologies have been used to manipulate cell-encapsulating hydrogels.	High spatial resolution, high throughput.	High complexity, medium potential adverse effects on cells, medium cell density.

2.1. Magnetic manipulation of cell-encapsulating hydrogels

Micro/nano-scale technologies have a significant impact on modern medicine.[43–47] To manipulate cells in micro/nano-scale volumes, magnetic fields have been exploited in a variety of ways including direct cellular manipulation, cell sorting, 3-D cell culture, local hyperthermia therapy, and clinical imaging applications.[43,48–56] For instance, magnetic fields have been utilized to manipulate cells to create 3-D tissue culture models

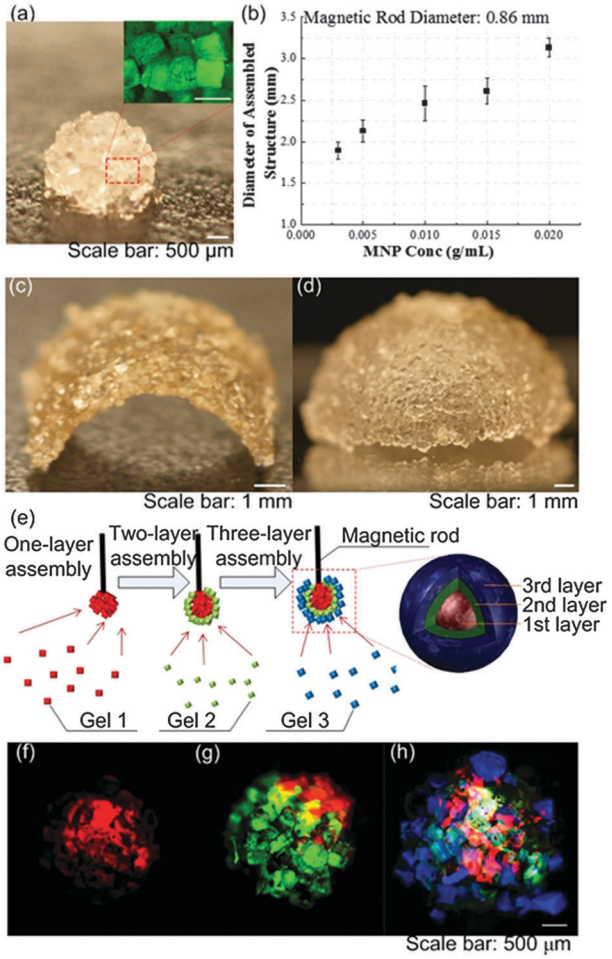

Fig. 1 Magnetic manipulation and assembly of cell-encapsulating hydrogels. (a) Magnified image of the assembled single-layer spheroid construct. (b) Maximum spheroid assembly size *versus* MNP concentration. (c) and (d) Images of engineered arc and dome constructs by employing a flexible surface. (e) 3-D assembly of fluoresencently tagged gels. Layers were stained with rhodamine-B (f), FITC-dextran (g), and TPB (1,1,4,4-tetraphenyl-1,3-butadiene) (h), respectively from inner to outer shell. *Reproduced with permission.*[7]

leveraging magnetic levitation.[57] Magnetic nanoparticles (MNPs) have been utilized to create two-dimensional (2-D) surface patterns,[43,58–60] as well as 3-D cell culture arrays[61] and characterize cell-membrane mechanical properties.[62] In these magnetic methods, cells were first mixed directly with ferrofluids or functionalized MNPs, and then exposed to external magnetic fields, allowing controlled manipulation. Besides, methods to encapsulate MNPs in hydrogels have been developed based on microfluidics[51,63–65] and applied to multiplexed bioassays, *e.g.* rapid sensing of nucleic acids.[66]

Assembly of cell encapsulating micro-scale hydrogels has been performed by utilizing MNPs (Fig. 1).[7] Gels were also shown to present paramagnetic properties without MNPs due to formation of free radicals during photocrosslinking.[8] These hydrogels were directed on a fluid reservoir by using a permanent magnet.[8] Magnetic transport of hydrogels can be affected by several factors including: (i) viscous drag, (ii) hydrogel–fluid interactions (agitations to the flow field), (iii) gravitational field, (iv) buoyancy force due to density difference, and (v) thermal effects. Here, it is assumed that the active forces are the magnetically-induced forces and fluidic drag forces. The motion of cell-encapsulating hydrogels can be modeled using Newton's law,

$$m\frac{\mathrm{d}\boldsymbol{v}_\mathrm{m}}{\mathrm{d}t} = \boldsymbol{F}_\mathbf{m} + \boldsymbol{F}_\mathbf{f} \quad (1)$$

where m and $\boldsymbol{v}_\mathrm{m}$ are the mass and velocity of the hydrogel, and $\boldsymbol{F}_\mathbf{m}$ and $\boldsymbol{F}_\mathbf{f}$ are the magnetic and fluidic drag forces, respectively. The magnetic force on a magnetized hydrogel by utilizing MNPs can be written as,

$$\boldsymbol{F}_\mathbf{m} = -V\mu_0(\boldsymbol{M}\cdot\nabla)\cdot\boldsymbol{H} \quad (2)$$

where V and $\boldsymbol{M}$ are the volume and magnetization of the hydrogel, respectively and $\boldsymbol{H}$ is the applied magnetic field. The fluidic drag force is approximated using Stokes' law for the drag on a sphere,

$$\boldsymbol{F}_\mathrm{f} = -6\pi\eta R_\mathrm{h}\boldsymbol{v}_\mathrm{m} \quad (3)$$

where η and $\boldsymbol{v}_\mathrm{m}$ are the viscosity and the velocity of the hydrogel, respectively. Using these active forces, kinematics of floating hydrogels can be predicted,[8] and assembly performance can be evaluated and improved.

2.2. Capillary driven manipulation of cell-encapsulating hydrogels

Lateral capillary forces were utilized for assembly of cell encapsulating micro-scale hydrogels,[4] and evaluated mathematically to assess the limitations that the size of objects imposes on the assembly process.[67] The assembly of two objects at the interface of two fluids (*e.g.*, air and mineral oil,[4] or two liquids[67]) can be evaluated by calculating the change in interfacial free energy. As two surfaces move from infinite separation to some finite separation, d (Fig. 2), the height h of the interface between the two objects can be calculated using the linearized Laplace equation:[67]

$$\frac{\partial^2 h}{\partial x^2} = \frac{1}{\gamma}(\Delta\rho g h - \Delta P_0) \quad (4)$$

where γ is the interfacial free energy, $\Delta\rho$ is the density difference between the two fluids, g is the gravitational acceleration, and ΔP_0 is the change in pressure across the interface at $x = 0$. The solution of eqn (4) is:[67]

$$h(x) = t\left[\frac{2}{1-\mathrm{e}^{(d/x_\mathrm{c})}} + \frac{\mathrm{e}^{(-x/x_\mathrm{c})} + \mathrm{e}^{(x/x_\mathrm{c})}}{\mathrm{e}^{(d/2x_\mathrm{c})} - \mathrm{e}^{(-d/2x_\mathrm{c})}}\right] \quad (5)$$

where x_c can be set as the capillary length $(\gamma/\Delta\rho g)^{1/2}$. The interfacial energy can be calculated as a function of distance between objects. The alteration in interfacial free energy, ΔW, can be set to $5\Delta l\gamma t$ (Fig. 2).[67] Results showed that interfacial free energy for capillary self-assembly is favorable for flat objects with thickness as small as 100 nm (Fig. 2).[67] For 2-D assembly of spherical objects, the radius of object at which interfacial free energy is close to thermal energy (kT) has been calculated to be on the order of 1 to 10 μm.[68,69]

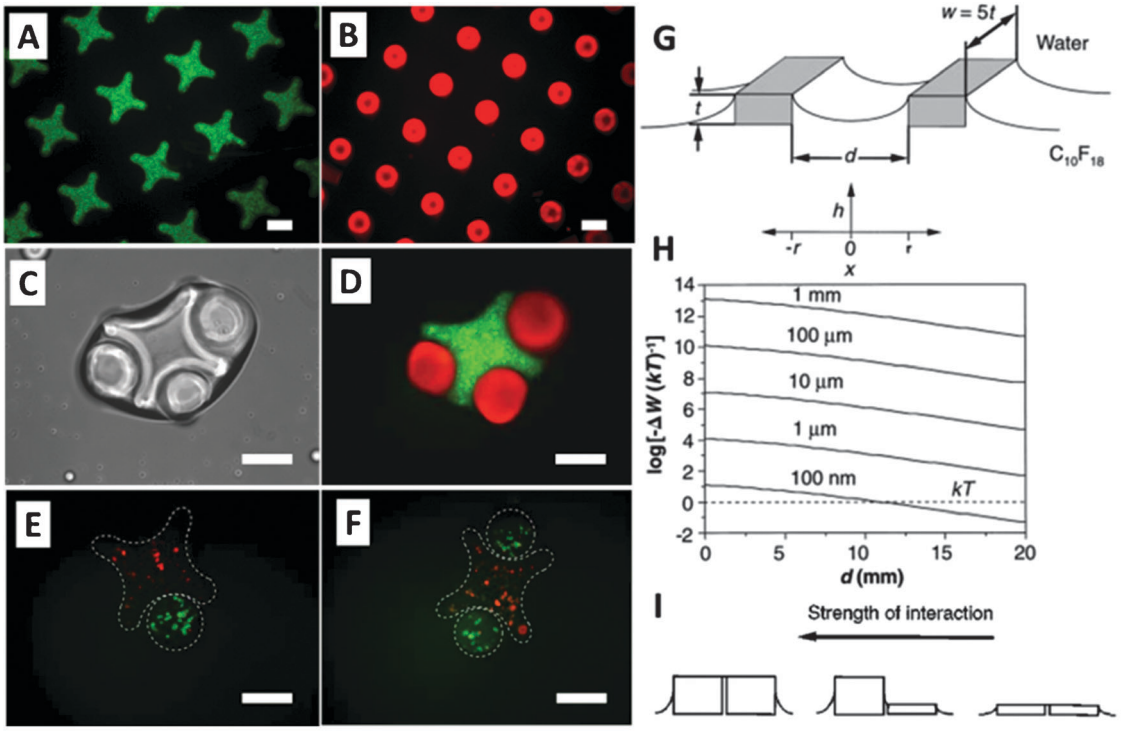

Fig. 2 Capillary driven manipulation and assembly of cell-encapsulating hydrogels. (A and B) Fluorescence images of cross-shaped and rod-shaped hydrogels stained with FITC-dextran and Nile red, respectively. (C) Phase-contrast image of lock-and-key assemblies with three rods per cross. (D) Fluorescence image of lock-and-key assemblies. (E and F) Fluorescence images of single rod and two rod assemblies (scale bars are 200 μm). (G) The schematic of two objects and the coordinate system for eqn (4) and (5). The objects have a height of t and a width of $w = 5t$, and their proximate surfaces are separated by d. (H) For a range of object height, t = 1 mm to 100 nm, the change in interfacial free energy (non-dimensionalized with thermal energy, kT) in bringing two surfaces from infinite separation to a finite separation, d, is plotted. (I) The strength of interaction is correlated with the height of capillaries. *Reproduced with permission.*[4,67]

2.3. Bioprinting cell encapsulating droplets

Droplet generation techniques based on microelectromechanical systems (MEMS) have been originally developed for applications in semiconductor industry.[70–77] To address the needs in complex tissue engineering applications, these techniques have also been used for cell encapsulation[17,78] and patterning (Fig. 3).[17,21,78] These technologies offer significant advantages over existing top-down scaffolding methods. Among the different techniques of bioprinting are acoustic,[17,79] inkjet,[80,81] valve-based,[47,78,82,83] and laser printing[13,22,84] technologies. For instance, cell-encapsulating picoliter droplets were acoustically generated from an open-pool without a nozzle, which eliminates challenges associated with nozzle shear or clogging (Fig. 4). These devices can eject a broad range of materials including viscous polymers, fluids and cells simultaneously from the same ejector array. Further, they offer micro-scale precision over the cell position with droplet directionality. Picoliter to nano-liter droplets (as small as 3–200 μm in diameter) can be generated with acoustic patterning technologies.[76,85]

Bioprinting can be divided into two steps: (i) formation of cell-encapsulating droplets from cell suspension, and (ii) impact and subsequent relaxation of droplets on the receiving surface. Cell encapsulation is a highly probabilistic phenomenon as there are several governing parameters such as cell density and cell distribution in suspension. Statistical methodologies can provide a better understanding of the cell encapsulation process. A reliable and repeatable control can be gained over the parameters that characterize the cell encapsulation process. For several target cell concentrations and types of cell loading, the encapsulation process was statistically analyzed.[86] As shown in Fig. 5A–C, while the percentage of target cells and homogeneity decreased in cell suspension solutions, the encapsulation probability of a target cell $P(X_t)$ decreased. More recently, a statistical model based on negative binomial regression has been also presented to demonstrate how (i) cell concentration in the ejection fluid, (ii) droplet size, and (iii) cell size affect the number of cells encapsulated in an ejected droplet.[87]

Similarly, for cell deposition, computational models enable researchers to develop an understanding of how parameters such as ejection speed and viscosity of cell suspension affect cell viability.[88–90] Mechanical factors, *e.g.*, shear stresses, hydrodynamic pressures, capillary forces, may amplify and cause deformation of cells. These factors can be controlled experimentally by adjusting ejection speed or by replacing cell suspension fluid with those having material properties (*e.g.*, viscosity, density, and surface tension) that lead to less shear stress on cells. Cell viability also depends on receiving surface characteristics such as hydrophobicity, roughness, and elasticity

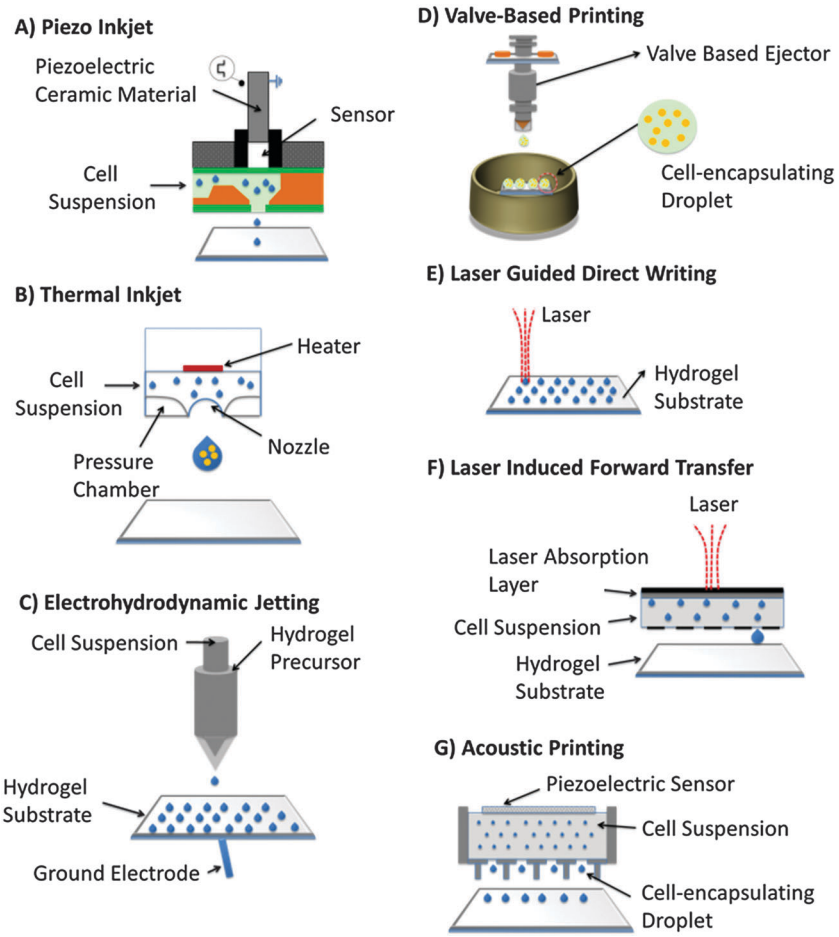

Fig. 3 Bioprinting technologies. (A) Piezo inkjet printing. (B) Thermal printing. (C) Electrohydrodynamic jetting. (D) Valve-based printing. (E) Laser guided direct writing. (F) Laser induced forward transfer. (G) Acoustic printing.

of the surface. Prediction of cell deformation and viability *via* computational methods can be complementary to fulfil several design goals for building complex viable tissue constructs. A finite difference front tracking model was developed to model the deposition of viscous compound droplets (*i.e.*, a smaller droplet encapsulated in a larger droplet) onto a receiving surface as a model for a cell printing process[89,91] (Fig. 5D–F). In this work, the settings that result in least cell deformation and the smallest rate of deformation were identified. The analyses were performed for a set of nondimensional numbers, *i.e.*, Reynolds number (Re), Weber number (We), viscosity ratio (μ_c/μ_d), surface tension ratio (σ_o/σ_i), diameter ratio (d_o/d_i), and equilibrium contact angle (θ_e). "Re" and "We" are nondimensional numbers in fluid mechanics to evaluate the ratio of inertial forces compared to viscous forces and surface tension, respectively.

The computational results demonstrated that cell deformation gradually increased as: (i) Re increased; (ii) d_o/d_i decreased; (iii) σ_o/σ_i increased; (iv) μ_c/μ_d decreased; or (v) θ_e decreased. On the other hand, a local minimum, at least, of maximum geometrical deformation was obtained at We = 2. Cell viabilities were linked to cell deformation by employing an experimental correlation of compression of cells between parallel plates[92] (Fig. 5F). Results showed that θ_e and μ_c/μ_d were highly correlated with cell viability.

3. Applications of micro-scale manipulation of cells

3.1. Diagnostic applications

The capability of manipulating cells (*e.g.*, capture/isolation) at the micro-scale level, in combination with rapid detection technologies, creates the potential for inexpensive, portable and disposable devices for POC testing. Particularly, there is an urgent need for such diagnostic tools in resource-constrained settings where well-trained technicians, basic laboratory infrastructure and sustained financial support are not available.[28,93,94] Additionally, patients would benefit from rapid healthcare technologies similar to rapid glucose tests. Such tests can enable close monitoring of patients suffering from a broad range of diseases ranging from renal diseases to infectious diseases such as HIV. Microfluidic technologies for cell manipulation in micro-scale volumes have enabled new approaches to monitor and detect various diseases. Here, we focus on (i) CTC capture and detection, (ii) $CD4^+$ T lymphocyte

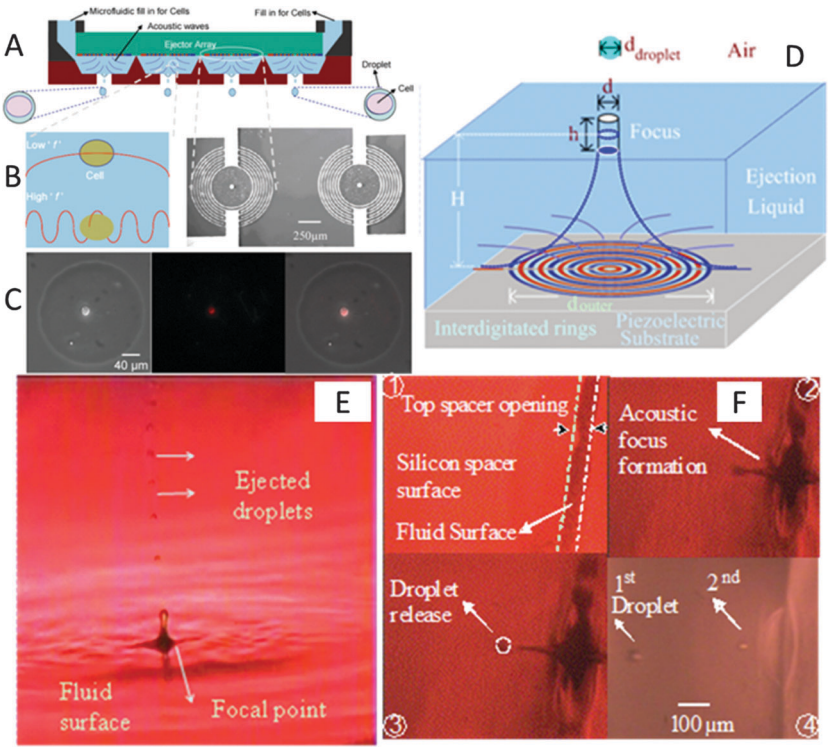

Fig. 4 Schematic for acoustic nozzles droplet generation technology. (A) Multiple ejectors and ejected cell encapsulating droplets from different reservoirs. (B) Comparison of acoustic wavelength with the cell diameter. (B) The interdigitated circular micromachined device. Scale bar is 250 μm. (C) Computerized printing of single cell encapsulating droplets *via* xyz stage control. (D) Cylindrical acoustic focus at the fluid surface. (E and F) 28 μm droplets ejected upward from an open pool. Droplets ejected downward from a 100 μm wide microfluidic channel spacer opening. The ejector generated single droplets drop-on-demand without satellites. *Reproduced with permission.*[17,71]

count in blood, (iii) pathogen detection and cancer biomarker detection, and (iv) sperm monitoring and sorting.

3.1.1. Capture/detection of CTCs in microfluidic devices. Cancer related deaths account for approximately 13% of all deaths each year,[95] primarily due to metastasis of CTCs in distant organs and subsequent metastatic diseases.[96] As such, isolation of rare CTCs (at a ratio of one cell per 10^9 blood cells) from whole blood can potentially achieve cancer detection and reduce cancer-related mortality, as well as provide target cells for molecular characterization, drug screening and treatment monitoring. Earlier, antibody coated magnetic beads have been used to develop a system to isolate and quantify CTCs from blood using the CellSearch System (Veridex LLC, Raritan, NJ).[97] Microfluidic devices have adapted this antibody-based isolation approach to isolate and enrich CTCs from peripheral blood.[25,98,99] Generally, microfluidic based approaches rely on the interactions between proteins on the surface of CTCs and corresponding ligands immobilized in microfluidic devices. Depending on the downstream applications, captured cells on-chip are subsequently subject to immunostaining and molecular analyses to provide biological insights into metastasis and to identify new biomarkers for anti-cancer treatment monitoring.

For example, isolation of CTCs from whole blood using a microchip was reported.[25] This microchip consists of microposts and the microchannel surface is coated with an anti-Epithelial cell adhesion molecule (EpCAM). On the surface of CTCs, the adhesion protein EpCAM is up-regulated compared to healthy blood cells. Under the optimal flow conditions, CTCs from metastatic lung, prostate, pancreatic, breast and colon cancer patients were captured on-chip due to the difference in the expression level of EpCAM.[25] The captured CTCs were subsequently immuno-stained for confirmation. Under controlled laminar flow conditions, the authors achieved capture efficiency of approximately 60% at a flow rate of 1–2 mL per hour and a purity of around 50%. With the advantage of continuous flow, this technology detected CTCs from 115 patients out of 116 in a study, indicative of the potential for management of cancer at clinical settings. This technology has been further developed by integrating an automated quantitative imaging system, which improved the analytical throughput.[99]

In addition to immunocapture, physical characteristics have been utilized for isolation of CTCs. CTCs are generally softer and more deformable than healthy cells,[100] which allows the detection of carcinoma cells using impedimetric transducers to measure the increase in volume of cancer cells under hypsometric pressure.[101] Alternatively, the size differences between cancer and benign cells can also be used to detect CTCs, based on conductance measurements.[102] These methods allow detection of cancer cells from whole blood without pre-labeling, potentially realizing serial monitoring of anti-cancer therapy at the primary care settings in the future.

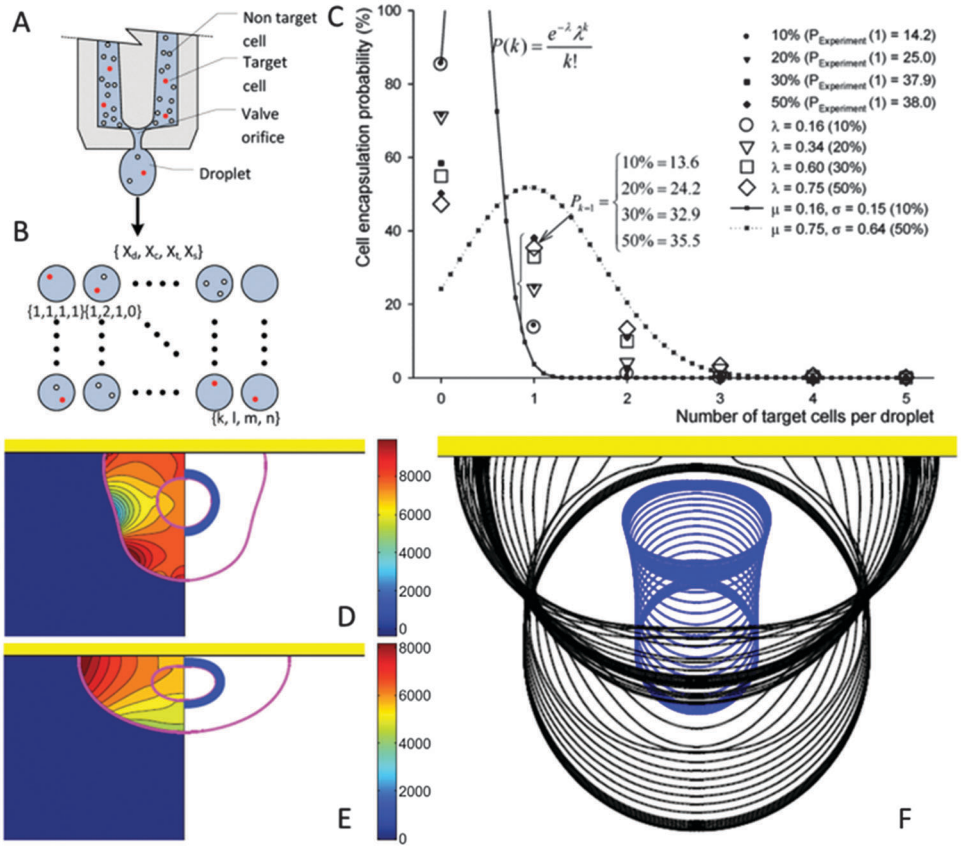

Fig. 5 Statistical and computational modeling of cell encapsulation and the printing process. (A–C) $P(X_t)$ (eqn (3.6) in ref. 86) are cell encapsulation probability functions for the heterogeneous cell mixture including several cell loading concentrations. (A) Heterogeneous mixture of target and non-target cells inside an ejector reservoir. (B) Four parameters were distributed onto a matrix: (X_d) the number of droplets that contain cells, (X_c) number of cells per droplet, (X_t) number of target cells, and (X_s) droplets encapsulating a single target cell. (C) Cell encapsulation probability, $P(X_t)$, as a function of number of target cells per droplet for cell concentration = 1.5×10^5 cells per mL. (D–F) Inner droplet representing the cell was assumed to be a highly viscous fluid and non-wetting (not sticking to the surface) while encapsulating droplets partially wetted the substrate. A moving contact line model[90,238] was utilized to predict the dynamic contact angle. (D and E) Pressure contours and pressure distribution on the cell were plotted at the left half and the right half, respectively. Shear stresses peaked in the vicinity of the triple point during the initial phase of droplet–surface interaction. Triple point is the point where outer droplets, receiving substrate and ambient air, coincide. Maximum pressure was located near the contact line just before recoiling, and migrated to the distal end from the receiving surface where it stayed there until the recoil phase. Governing non-dimensional numbers are: We = 0.5, Re = 30, d_o/d_i = 2.85, σ_o/σ_i = 2541, μ_c/μ_d = 10. (F) Sequential impact images of cell encapsulating droplets. *(A–C) are reproduced with permission[86] and (D–F) are reproduced with permission.*[89]

Captured CTCs can also be coupled with molecular techniques to monitor the regulation of protein expression that is associated with cancer metastasis. For example, the overexpression of epidermal growth factor receptor gene (EFGR) has a high correlation with cancer metastasis.[103] In a small cohort study, genomic analysis of those isolated CTCs from non-small-cell lung cancer patients was performed.[98] It was observed that the number of isolated CTCs was highly correlated with therapeutic responses and/or tumor progression. Particularly, the emergence of EGFR mutations was identified in some cases with progressive tendency. Constant molecular monitoring of cancer patients receiving treatment has potential to provide valuable information on prognostics and treatment efficacy.

3.1.2. CD4$^+$ T lymphocyte count. CD4$^+$ T lymphocyte cell count has been widely used as a gateway method to enroll acquired immune deficiency syndrome (AIDS) patients to initiate antiretroviral therapy (ART) in developing countries. Although there are significant advances in developing preventative microbicide vehicles,[104–110] HIV/AIDS has caused 25 million deaths worldwide since the first case was reported in 1981.[111] HIV primarily infects host immune cells such as CD4$^+$ T lymphocytes and leads to immunodeficiency syndrome. Over time, CD4$^+$ cell count gradually decreases and this reflects the host immune status against HIV replication. The World Health Organization (WHO) guidelines recommend a clinical cutoff of 350 cells per μL to initiate ART and/or switch effective treatment regimens if immunological failure occurs. Although commercial flow cytometers can be used to measure CD4$^+$ cell count, prohibitive cost of instruments, consumables, and maintenance challenges significantly limit the wide use of CD4$^+$ cell count to initiate ART in developing countries.[112] In addition, CD4$^+$ cell count needs to be monitored regularly to evaluate treatment response and patient adherence. Without regular monitoring (*e.g.*, average every 4–6 months), HIV may evade effective drug suppression and lead to emergence of drug-resistant strains in infected individuals, which thus

facilitate the spread of drug-resistant strains in the extended population. Clearly, there is an urgent need to develop rapid, simple and inexpensive POC CD4 assays to control the AIDS pandemic in resource-constrained settings.

So far, a variety of $CD4^+$ cell counting methods have been implemented using microfluidic devices,[26–28,44,113] which require precise manipulation of blood on-chip. The common approach employed by these devices is to capture, isolate and detect $CD4^+$ T lymphocytes with a combination of mechanical, electrical, optical and cell-adhesion mechanisms. $CD4^+$ T lymphocytes can be captured with efficiency up to $70.2 \pm 6.5\%$ in a straight microchannel *via* the aid of anti-$CD4^+$ antibody immobilized on the device surface. For rapid detection, the captured $CD4^+$ T lymphocytes can be stained using two specific biomarkers, $CD4^+$ and $CD3^+$ molecules, on the cell membrane. By dual-labeling, $CD4^+$ T lymphocytes can be detected under a fluorescence microscope, and the number of $CD4^+$ T lymphocytes can be counted manually under an optical microscope. To speed up the detection process, automated counting methods that use image recognition algorithms were developed.[26,28,114] These algorithms enabled 100 times faster outcomes than manual counting for the fluorescent stained cells, especially when a large number of cells are present in the microchannels on the order of thousands. These approaches significantly increase the efficiency and accuracy to obtain $CD4^+$ cell count. However, it should be noted that the need for a fluorescence microscope is not practical for POC testing in resource-constrained settings. To address this barrier, new technologies were developed including shadow-based lensless imaging,[26–28,112,115] electrical sensing of lysed cells after isolation[116] integrated with microfluidic chips where the cells were selectively captured. These advances led to point-of-care microfluidic detection methods that provide a $CD4^+$ count using fingerprick volume of whole blood without any sample preprocessing steps.[26] Specifically, to suit the need in resource-limited settings, label-free detection and counting strategies have been developed using light microscopy, impedance measurements and lensless imaging. In an initial effort, a light microscope was used to count captured $CD4^+$ cells in a microfluidic device which involves a tedious manual counting step.[117] To overcome this drawback, a rapid $CD4^+$ cell counting method was developed using impedance measurement.[118] This method eliminated the need for a fluorescence microscope and significantly shortened the quantification time as required in manual counting, which can be potentially implemented at the POC settings. Recently, $CD4^+$ cell counts can be obtained using a lensless, ultra wide-field cell array based on shadow imaging (LUCAS) (Fig. 6),[112] which enables rapid $CD4^+$ cell counting within 10 minutes.[27] Further, the LUCAS system has been validated in Tanzania with clinical samples and the results show positive correlation with the gold standard, *i.e.*, flow cytometry, showing the potential of pairing with POC testing to facilitate clinical on-site decision-making.[26]

3.1.3. Microfluidics based POC applications. Similarly, microfluidic devices can also be used to detect multiple pathogens such as bacteria and viruses as well as smaller molecules

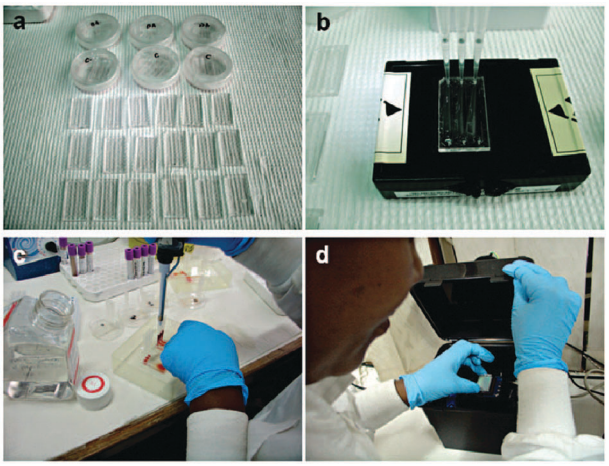

Fig. 6 Microfluidic CD4 cell count performed by minimally trained personnel at MUHAS. (a) Microfluidic chips. (b) Preparation of surface chemistry with antibody injection. (c) Injection of blood sample. (d) Lensless imaging detection of CD4 cell count on-chip. *Reproduced with permission.*[26]

such as proteins, demonstrating the versatility for developing POC assays in a miniaturized format. For example, microchips have been developed to selectively capture *E. coli* from various samples such as whole blood, phosphate buffered saline (PBS), milk, and spinach.[119] This method can be used to monitor potential food poisoning and open wound infections without using conventional bacterial detection methods such as agar plate culture or polymerase chain reaction, as these conventional methods are time-consuming and instrument-dependent. In addition, agar plating, the gold standard for bacterial detection, requires 48 to 72 hours to complete,[120] and it is often associated with false negative results ranging from 7.2 to 21.2%.[121,122] The immuno-based microchip captured *E. coli via* lipopolysaccharide binding protein with a detection limit of 50, 50, 50, and 500 CFUs per mL in PBS, blood, milk, and spinach samples, respectively. The presented technology can be broadly applied to detect other pathogens, creating new avenues for POC diagnosis and monitoring of infectious diseases.

Enabled by the reliable immuno-capture of pathogens in microfluidic devices, this technology was extended to address the urgent need for developing rapid HIV viral load assays, which is essential to diagnose early HIV infection and monitor AIDS patients on antiretroviral therapy (ART).[94] Also, HIV viral load assays can be used to prevent mother to child transmission (MTCT), since traditional immunoassays cannot reliably detect HIV infection in infants until the age of 18 months due to passively transferred maternal antibodies.[123] Previously, an on-chip detection method was developed to selectively capture HIV from 10 μL unprocessed HIV-infected patient whole blood.[124] The method leveraged the photo-stability of quantum dots (Qdots) and tagged the captured HIV particles with dual-color labeling. Two types of Qdots (Qdot525 and Qdot655) were used to label envelope glycoprotein gp120 and high-mannose glycans for dual-staining. Recently, the on-chip capture mechanism was used to capture various HIV subtypes[125] that are dominant in developing countries and constitute a significant

challenge for commercial Ribonucleic acid (RNA) viral load assays.[126,127] The results showed that anti-gp120 antibodies immobilized *via* Protein G surface chemistry captured subtypes A, B and C spiked in whole blood with efficiencies of 73.2 ± 13.6, 74.4 ± 14.6 and 78.3 ± 13.3% at a viral load of 1000 copies per mL, and with efficiencies of 74.6 ± 12.9, 75.5 ± 6.7 and 69.7 ± 9.5% at a viral load of 10 000 copies per mL. In another recent study, an on-chip sample preparation method that can remove blood cells from whole blood based on size-exclusion was developed.[128] This lab-on-a-chip filter (2 μm pore size) device isolated HIV at high recovery efficiencies of 89.9 ± 5.0%, 80.5 ± 4.3% and 78.2 ± 3.8%, for the clinically relevant viral load levels of 1000, 10 000 and 100 000 copies per mL, respectively, while retaining 81.7 ± 6.7% of red blood cells (RBCs) and 89.5 ± 2.4% of white blood cells (WBCs) on the filter membrane. The chip can be operated by a single manual pipetting step without requiring any sample pre-processing steps. These devices can be potentially integrated with other detection mechanisms such as RT-PCR or enzyme-linked immunosorbent assay (ELISA) to achieve sample-in answer-out for HIV viral load monitoring and early diagnosis in resource-constrained settings. Recently, an electrical sensing method was developed to measure the impedance change resulted from the HIV viral lysate in a disposable microchip, which showed promising results for the detection of multiple HIV-subtypes including A, B, C, D, E, G, Panel at an early stage.[40]

Additionally, microfluidic devices can be used to miniaturize conventional laboratory-based detection methods such as ELISA to detect protein biomarkers.[129,130] For instance, ovarian cancer is asymptomatic at the early stages and it often leads to a poor 5 year survival rate of 33% at stages III and IV, when patients present with symptoms.[131] To address the urgent need for ovarian cancer detection, an ELISA microchip was developed to detect human epididymis protein 4 (HE4) from urine.[130] The microchip ELISA results were detected using a cell phone *via* integration of a mobile application that reports the concentration of HE4 on a phone screen (Fig. 7). As shown, the level of HE4 in urine samples from cancer patients (n = 19) detected was significantly elevated than the healthy controls (n = 20) ($p < 0.001$). Receiver operating characteristic (ROC) analyses showed that the microchip ELISA had a sensitivity of 89.5% at a specificity of 90%. This approach offers a quantitative ELISA test using a simple cell phone based colorimetric detection instead of an expensive, bulky spectrophotometer, thus potentially offering an attractive POC platform. In addition, the use of multi-channel microfluidic design allows detection of multiple biomarkers simultaneously, as well as the control.

3.1.4. Microfluidic based sperm monitoring and sorting for reproductive medicine. 6.1 million American couples (approximately 10% of American couples of childbearing age) are affected by infertility.[132] Male originated issues are reported in almost half of the infertility cases, which require evaluation

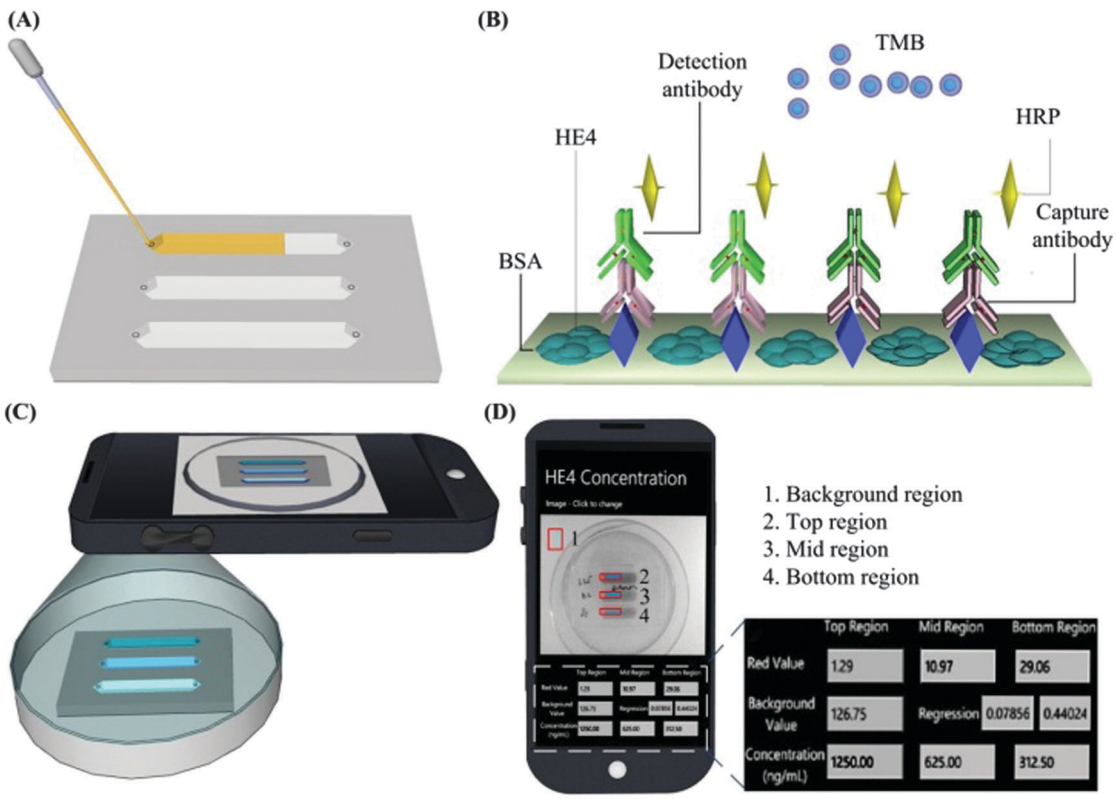

Fig. 7 Microchip ELISA integrated with cell phone application for detection of ovarian cancer from urine. (A) Loading of a small volume (100 μL) of urine sample into the microchannel. (B) Principle of direct ELISA for detection of HE4 on-chip. (C) The color development in microchannels was imaged using a cell phone built-in camera. (D) The concentration of HE4 in urine reported on the cell phone screen *via* a mobile application. *Reproduced with permission.*[130]

of parameters defining sperm quality, such as motility and sperm count. To address male based infertility issues, *in vitro* fertilization (IVF) with or without intra cytoplasmic sperm injection (ICSI) has been the most preferred assisted reproductive technology (ART) in clinics. One of the challenges of IVF and ICSI is identification and isolation of the most motile and the healthiest sperm from semen samples that have poor sperm counts (*i.e.*, oligozoospermia) and/or poor motility (*i.e.*, oligospermaesthenia).

The applications of micro/nano-scale technologies to reproductive medicine have been explored.[115,133–137] Microfluidic technologies have been employed to separate motile sperm with a higher efficiency compared to conventional sperm sorting techniques.[115,134–139] A microfluidic device with an outlet junction was developed to separate motile sperm from directionally moving non-motile sperm.[138] More recently, a lensless imaging system was integrated with a microfluidic chip to achieve automatic and wide field-of-view (FOV) imaging of a small population of sperm inside a microfluidic channel (Fig. 8).[115] Using a lensless charge-coupled device (CCD) system, sperm swimming inside a channel were directly imaged as shadow patterns and sperm movements were tracked (Fig. 8). Since the field of view of the lensless sensor (4 mm × 5.3 mm) is approximately 20 times that of a conventional 10× objective lens (1 mm^2), sperm stay within the field of view. Further, larger CCD systems (37.25 mm × 25.70 mm) have been earlier shown to reliably detect immobilized cells in microchannels.[27,112] These systems could be used to record sperm over an entire channel and even in multiple parallel or serial channels. As the sperm is known to be responsive to gravitational stimuli,[140] sperm motion in both horizontal and vertical microchip configurations was recorded, and results were displayed in bull's eye plots presenting the sperm movement on chip (Fig. 8L). In both configurations, sperm displayed great diversity in their patterns of motion and direction. The swimming paths were tracked and the kinematic parameters that define sperm motility, including average path velocity (VAP), straight-line velocity (VSL) and straightness (VSL/VAP) were quantified (Fig. 8M).

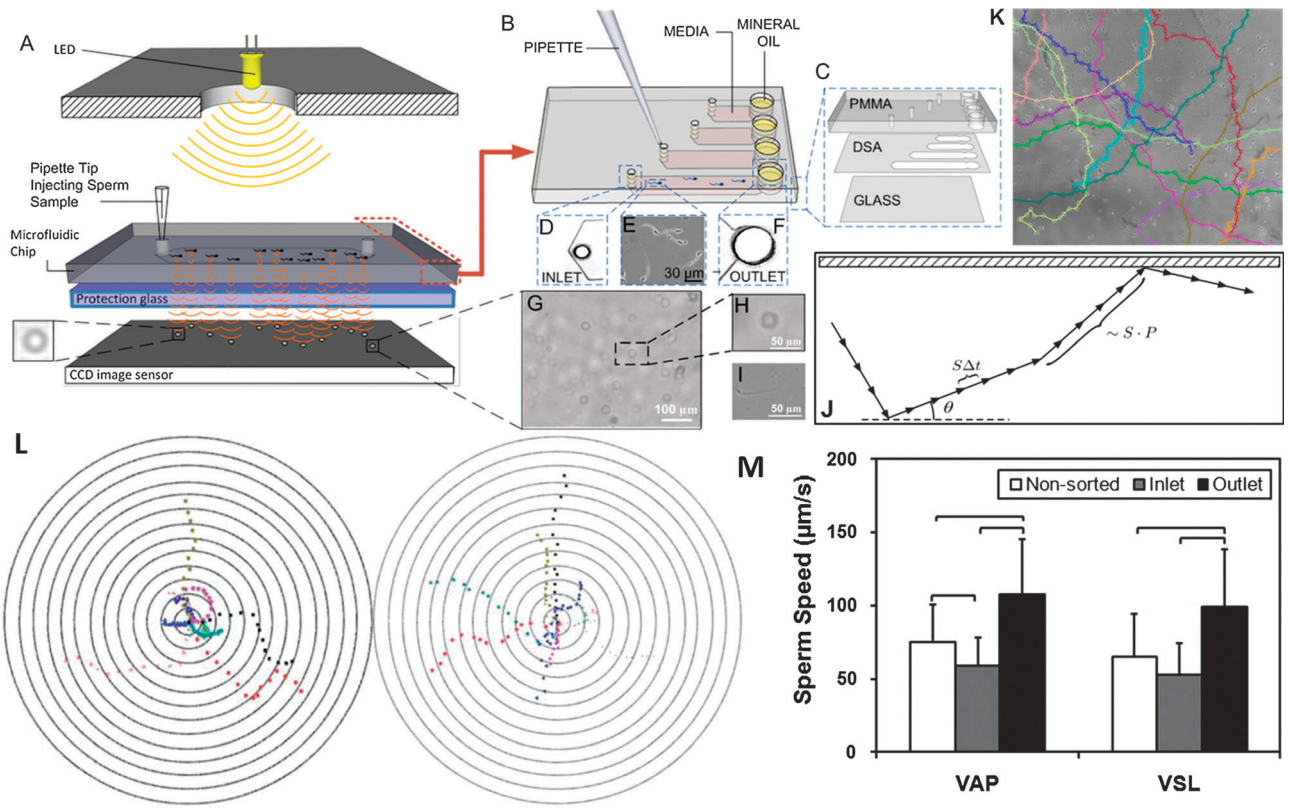

Fig. 8 Sperm sorting. (A) Lensless imaging platform (LUCAS) integrated with a microchip for sperm tracking as highlighted by Nature Photonics.[239] Shadows of the sperm generated by diffraction can be imaged using CCD in one second. (B) Loading sperm samples into microchannels of the space-constrained microfluidic sorting (SCMS) system from the inlets. The SCMS system with different channel lengths is assessed for effective sperm sorting. (C) The chip has three layers: PMMA, double-sided adhesive film (DSA), and glass coverslip. (D) Image of the channel inlet with a diameter of 0.65 mm under a 2×. (E) Image of sperm swimming inside a microchannel under a 10× objective. (F) The channel outlet with 2 mm diameter viewed using a 2× objective. (G–I) Sperm shadows on LUCAS. (J) A schematic of the trajectory of a sperm performing a Persistent Random Walk (PRW), where S is the velocity, P is the persistence time, Δt is the time step, and θ is the angle the trajectory makes with the x-axis. (K) Sperm tracks from image analysis. (L) Bull's eye plot showing sperm motility vectors in the horizontal (left) and vertical (right) configurations. The distance between the adjacent concentric circles is 100 μm. (M) Comparison of Average Path Velocity (VAP) and Straight Line Velocity (VSL) of sperm for non-sorted conditions, and at the inlet and outlet of the 7 mm long microfluidic channel. The VAP and VSL were observed to be significantly greater for the sperm cells imaged at the outlet of the microfluidic channel compared to non-sorted sperm and the sperm at the inlet. Therefore the microfluidic sperm tracking system presented here shows potential to be also used as a sorting platform (n = 33–66, brackets indicate statistical significance with $p < 0.01$ between the groups). *Reproduced with permission.*[115]

VAP refers to the average distance that a sperm covers in the direction of movement per unit time. VSL is the ratio of the straight-line distance between the start and end points of a sperm trajectory to the elapsed time until the sperm reaches the end point. Sperm were tracked in both horizontal and vertical configurations and the motilities were measured. The microfluidic channels create an environment that mimics the natural swim paths of sperm. Under real physiological conditions, sperm move through the vaginal mucus, cervical mucus and the cervical canal similar to a microfluidic channel. Once the mucus on the vaginal surface transforms into a less viscous watery phase, microchannels are formed. Such a space constrained microenvironment (*i.e.*, the length scale in the flow direction is significantly larger than that in other directions) directs sperm towards the oocyte along with other contributing factors such as chemotaxis.[115] To demonstrate microchip-based sperm sorting, sperm motilities at the outlet and inlet were compared to that of non-sorted sperm controls. As shown in Fig. 8M, sperm motility at the outlet was significantly higher than those of non-sorted sperm ($p < 0.01$), indicating that the microchip can be used to sort the most motile sperm, which can then be collected from the outlet. In addition, given the wide range of sperm velocities even after sorting, single cell based processing and monitoring enables separation of highest quality motile sperm from the rest utilizing either vertical or horizontal configurations. Recently, the exhaustion of mouse sperm (30 min) and human sperm (>1 hour) were quantitatively demonstrated and experimentally validated using microfluidics as an enabling technology.[141]

3.2. Applications in isolation, purification, and enrichment of cells

Isolation, purification and enrichment of rare and specific target cells from heterogeneous populations and manipulation of cells in micro-scale volumes have enabled advancement of fields such as: cell based diagnostics,[27,29,117] genomic and proteomic analyses,[25,142,143] clonal and population studies,[144,145] stem cell isolation for tissue engineering,[29,30,146,147] and circulating tumor cell isolation for cancer research.[25,148] Fluorescence-activated cell sorting and magnetic-activated sorting are commonly used cell manipulation technologies for isolation, which require preliminary processing and labeling of cells with fluorophore or magnetic particle conjugated antibodies. While these methods are powerful and successfully separate cells from heterogeneous mixtures, the cost, complexity and requirements for infrastructure (*e.g.*, facility and reagents) limit their use.[149] Miniaturization of these systems has been attempted by reducing them to simpler microfluidic versions.[150,151] However, the required peripheral equipment still remains large in size and costly. Furthermore, genomic studies on captured cells in microfluidic systems are mainly hampered by the loss of genomic material, which can adhere to the channel walls due to the large surface to volume ratio. These limitations can be addressed by the release and downstream processing of captured cells in microfluidic channels through manipulation in micro-scale volumes.[29,30]

Release of the selectively captured live cells (*e.g.*, CTC, $CD4^+$, $CD34^+$, endothelial cells) in micro-scale volumes would enable post-culturing, clonal and molecular characterization studies. However, challenges remain in effectively releasing the captured cells in microfluidic channels without compromising the viability of the captured cells.[152–154] To minimize adverse effects on cells, manipulation and recovery of the captured cells need to be performed without using chemical or physical factors, which can affect cellular characteristics. For example, using enzymatic or fluid shear based detachment is known to adversely affect cell viability and function.[155,156] Alginate based hydrogels have recently been used in combination with poly(ethylene glycol) and conjugated antibodies in microfluidic channels to capture endothelial progenitor cells from blood.[157] The captured cells were then released by dissolving the hydrogel in the channels with a chelator, *e.g.*, ethylenediaminetetraacetic acid (EDTA). Alginate hydrogels, however, allow a high level of non-specific binding[154,158] and offer limited numbers of sites for the conjugating antibodies, which significantly reduce the capture efficiency.[157] Furthermore, coating and chelation of hydrogels in microfluidic channels add extra steps and cost, lengthy processing time, operational complexities and additional reagents, which render this approach challenging to apply, especially at the bedside or resource-constrained settings.

Most of the downstream applications of cell capture require the captured cells to be lysed on-chip for genomic and proteomic analysis. However, cellular materials are lost to the microchannel surfaces due to the large surface to volume ratio. Additionally, in most cases the captured cells are so rare in concentration that they need to be expanded over culture for following biological analysis steps. Hence, manipulation and release of captured cells in microfluidic channels is a significant enabling biotechnology with broad applications. It was previously shown that poly(*N*-isopropylacrylamide) (PNIPAAm) coated surfaces interact strongly with peptides and proteins (*e.g.*, insulin chain A, serum albumin) above lower critical solution temperature (LCST).[159,160] Whereas, when the temperature of the surface is reduced below the LCST, a complete desorption of the adsorbed proteins is possible.[159,160] It was shown that the protein adsorption–desorption mechanism on a temperature-responsive polymer (PNIPAAm)[160] can be modified to develop a biotin-binding protein and biotinylated antibody based surface chemistry to rapidly and selectively capture and controllably release cells on-demand in microfluidic channels.[29,30] Thermoresponsive microfluidic channels were developed by functionalizing surfaces with biotin-binding protein and biotinylated antibody that can selectively capture specific cells from blood and controllably release with high viability and specificity, which provide a new platform to manipulate cells in micro-scale volumes (Fig. 9). More recently, a microfluidic system with sufficient micro-scale control to locally release a selected set of captured cells on-chip would significantly increase specificity (Fig. 10).[30] As microfluidic cell capture methods suffer from non-specific binding events, being able to manipulate and selectively release the undesired or desired

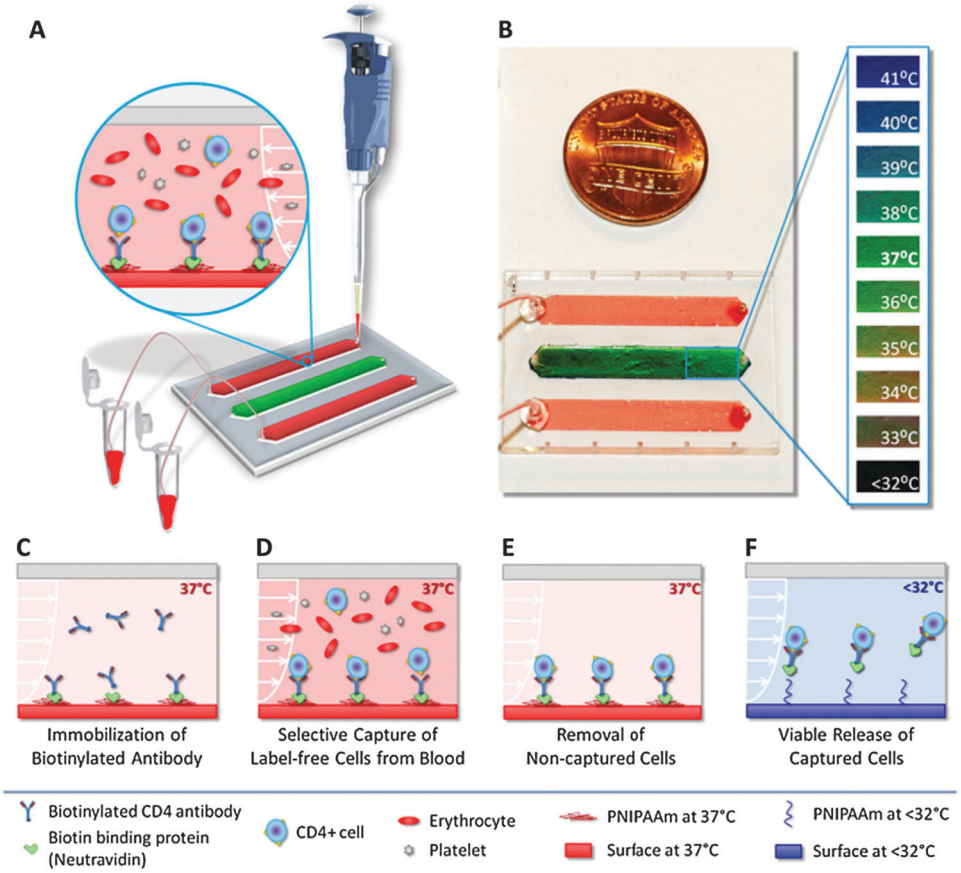

Fig. 9 Isolation, purification, and enrichment of cells using thermoresponsive microfluidic channels for on-demand releasing the selectively captured cells from heterogeneous mixtures.[29] (A) The thermoresponsive microfluidic chip is composed of three channels. The middle channel was used as an indicator of the temperature. (B) The indicator channel was covered with liquid crystal dye. (C) Schematic representing the mechanism of label-free selective capture of cells and on-demand release of cells in thermoresponsive microchannels. (D) Sample at 37 °C (*e.g.*, blood) is injected into the channel, and the target cells (*e.g.*, $CD4^+$ or $CD34^+$ cells) are captured. (E) The non-target cells in channels, which are not captured, are then washed off. (F) The channels are then cooled down below 32 °C. Upon cooling, the released cells are rinsed off the channels and collected at the outlet. *Reproduced with permission.*[29]

cells in channels[30] would improve the purity of captured cells especially for subsequent genomic/proteomic analysis[161] and biomarker discovery.[162]

3.3. Applications in tissue engineering and regenerative medicine

Cells in tissues and organs are intricately organized in a 3-D architecture at high densities. The capability to precisely position individual cells in a 3-D architecture at high densities can contribute to recapitulation of more physiologically similar tissues through manipulation of cells in micro-scale volumes. Over the years, there have been significant efforts to generate tissue-engineered organs.[163–172] The following characteristics of native tissues can be mimicked by employing technologies to manipulate cells in micro/nano-scale volumes: complex 3-D cellular and extracellular architecture, high cell density and complex vascular network. A crucial aspect of tissue engineering is to reproduce the body's architectural intricacies that would facilitate the vital cell–cell and cell–extracellular matrix (ECM) interactions in creating an *in vivo*-like environment.[173–178] Current methods for generating 3-D tissue constructs offer a limited control over cell density, which is well below the physiologically relevant densities.[22] For instance, cardiac tissue is comprised of a high density of cardiomyocytes, cardiofibroblasts and endothelial cells ($\sim 10^8$ cells per cm^3).[179] There is a need for a nutrient and oxygen rich environment for the cells residing deep in tissues. Therefore, a crucial challenge in tissue engineering of organs is to supply sufficient oxygen and nutrients to sustain cells located deep within the 3-D tissue construct with a porous or vascular network.[180–182] Current engineered 3-D tissues are developed to culture cells within biodegradable natural or synthetic scaffolds.[164,183–186] These engineered scaffolds function as 3-D structures within which cells grow, interact with the ECM and communicate with other cells in the proximity.[164,187] Scaffolding techniques have traditionally been used to form degradable porous, polymer scaffolds (*e.g.*, polyethylene glycol, collagen hydrogels and agarose) that are seeded with cells forming a 3-D construct.[163,188–190] Even though these methods are commonly used, scaffold-based technologies face challenges in precisely patterning cells in specific architectures to form highly organized and high cell density tissue constructs. Stepwise brick-by-brick building

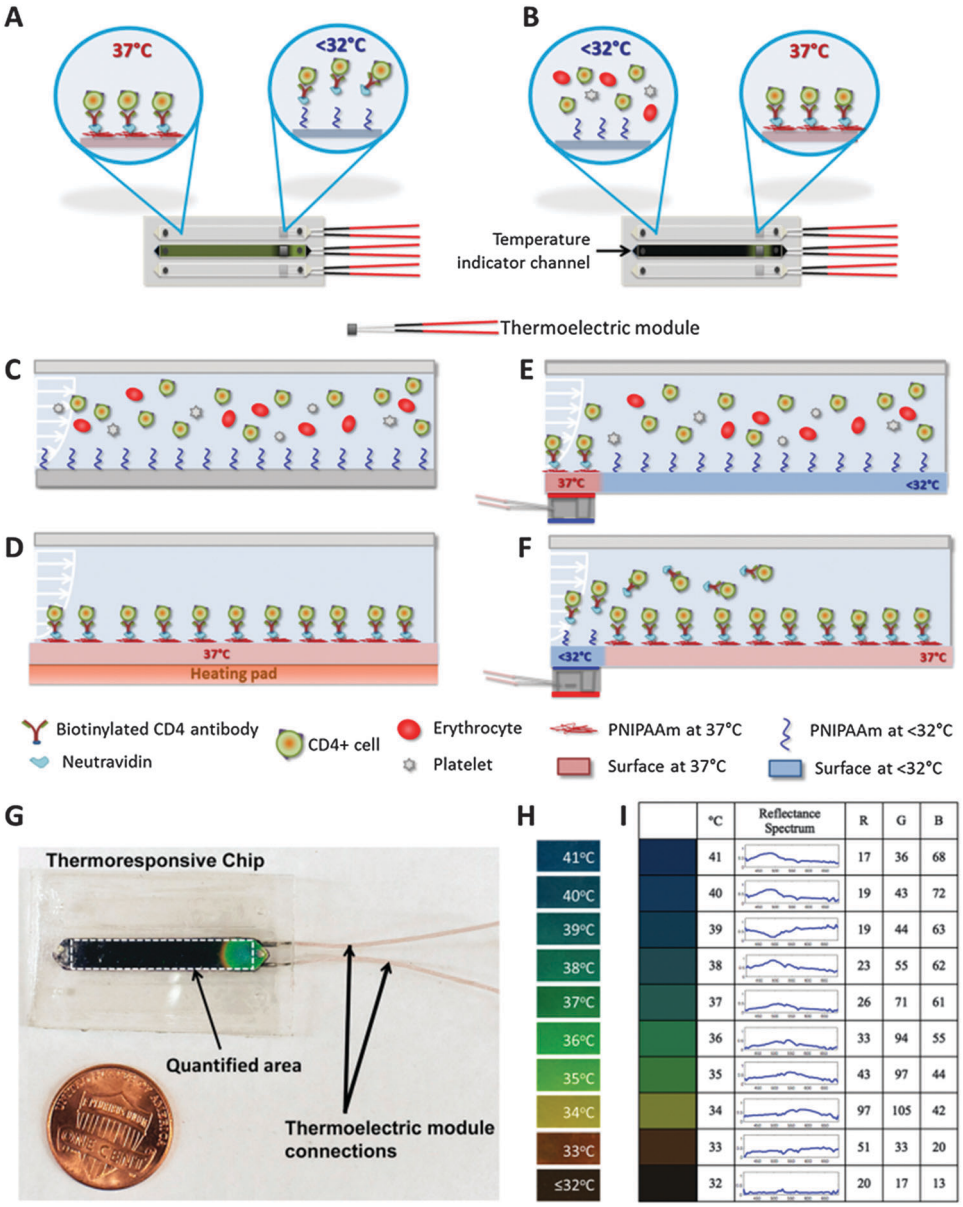

Fig. 10 Manipulation of cells in microchannels through local capture and on-demand release. (A) Local release of captured cells. (B) Local capture of specific cells in microchannels. (C–F) Mechanism of local manipulation of cells in microchannels in the absence and presence of thermoelectric heating elements. (G) Local control of temperature thermoresponsive microchannels and a photograph of a microchip with a local temperature control. (H) Temperature responsive dye works between 32 °C to 41 °C, and displays green color at 37 °C, the temperature at which cells were captured. The dye appears black below 32 °C, at which on-demand local cell release is achieved. (I) Baseline RGB values represent the colors displayed by the temperature indicator channel. *Reproduced with permission.*[30]

block techniques constitute an alternative approach to build 3-D tissue constructs.[190] In this approach, 3-D tissue structures are built by using micro-scale hydrogels (200–500 μm in size).

Various bioprinting methods have been developed to control cell seeding in 2-D and 3-D settings, such as inkjet and laser printing[21,80,81,191] to gain control over the spatial cellular and ECM composition, cell viability and functionality, and spatial density.[192] Cell manipulation technologies in micro-scale volumes can have a clinical impact on medicine, such as in cardiac and neural tissue regeneration. Cardiovascular diseases affect 70 million Americans, resulting in an economic burden of $300 billion and accounting for nearly 40% of all deaths in the US.[18] Conventional treatments of cardiac injury cannot achieve myocardial regeneration. Engineered cardiac tissue grafts can be surgically placed into the defect site to facilitate cardiac regeneration.[18] Additionally, neurodegenerative diseases,[193–196] such as Parkinson's disease (PD), Alzheimer's disease (AD), Huntington's disease (HD), Amyotrophic lateral sclerosis (ALS), and Traumatic brain injury (TBI), lead to impairment of the neural system, loss of cognitive abilities, and permanent paralysis. Currently, there is no effective treatment for neurodegenerative diseases, or brain and spinal cord injuries.[197,198] Neural tissue is extremely complex, contains many different cell types with connections forming an intricate

network. The neural circuits of the brain are 3-D networks that are diverse in cellular and molecular composition, as well as morphology. For example, for brain tissue engineering, which has thousands of different kinds of cells arranged in complex 3-D organization, new kinds of engineering techniques and micro-scale cell manipulation methods are required.[42,199–203]

3.4. High-throughput *in vitro* drug testing applications

Cell microarrays have been widely used to screen for drug candidates in a high-throughput manner.[23] Compared to traditional screening methods in a 384-well plate, cell microarrays have advantages such as reduction of reagent consumption and shortened assay time. In a typical cell microarray, high-density cell spots are deposited *via* micro-scale cell manipulation methods (*e.g.*, bioprinting, soft lithography) with precise temporal and spatial control. To test the drug efficacy and toxicity on cell microarrays, millions of drug candidates can be screened simultaneously. As reported, a variety of methods have been developed to deposit cells in micro-scale volumes onto microarrays, including patterning,[204] stamping,[205] microfluidic-based drug loading[206] and aerosol sprays.[207,208] These studies clearly demonstrated the widespread applications of 3-D cell microarrays for drug screening with significantly increased cost-effectiveness.[209–212]

3.5. Applications in biopreservation and cryoprinting

Biopreservation aims to preserve cells and tissues by cooling them to sub-zero temperatures at which biological activity is slowed down or completely ceased.[213,240] Following the cryopreservation time of interest, frozen tissues and cells are thawed, and ideally samples resume to their biological activity. During this process, cryoprotectant agents (CPAs) are employed to avoid cryoinjury of cells by cooling to temperatures at which intracellular ice formation takes place. The current practice for cryopreservation are slow freezing and vitrification using various CPAs such as dimethylsulphoxide (DMSO), 1,2-propanediol (PROH) and ethylene glycol (EG), sucrose, trehalose and mannitol. The slow freezing approach[214] is an established method, in which samples are cryopreserved at controlled freezing rates. Low levels of CPAs are used (*e.g.*, 1.5 M) in the slow freezing method to avoid intracellular ice formation and minimize cell membrane[215] and cytoskeleton damage.[216] However, this technique is not ideal due to the low post-thaw cell survivability and functionality. On the other hand, vitrification transforms cells into a glass-like solidification state,[217] and has emerged as a potentially ideal alternative method because of the higher survival rate by eliminating ice crystal formation. However, high levels of CPA (*e.g.*, 6–8 M) have to be used for rapid freezing necessary for vitrification (*e.g.*, $-1500\ ^{\circ}C\ min^{-1}$), which may also cause uncontrolled differentiation and smaller viability of cells.[218–220]

Integration of nano-liter droplet cell encapsulation technologies with vitrification is promising.[221–223] Single to few cells encapsulated in droplets can be directly ejected into a liquid nitrogen reservoir utilizing bioprinting technologies for vitrification. These droplets can also be placed on a thin film and then directly dipped into liquid nitrogen.[224] This process enables minimized CPA volumes for vitrification, and, hence, benefits from enhanced warming and cooling rates due to the larger surface to volume ratio. Moreover, biopreservation technologies may need to achieve processing of large sample volumes at high-throughput to enable clinical relevance and practical use. For instance, the cryopreservation of blood is of great importance to public health during natural disasters, global issues, warfare, and in clinical settings due to fluctuations in supply and demand.[225] Also, the existing approaches

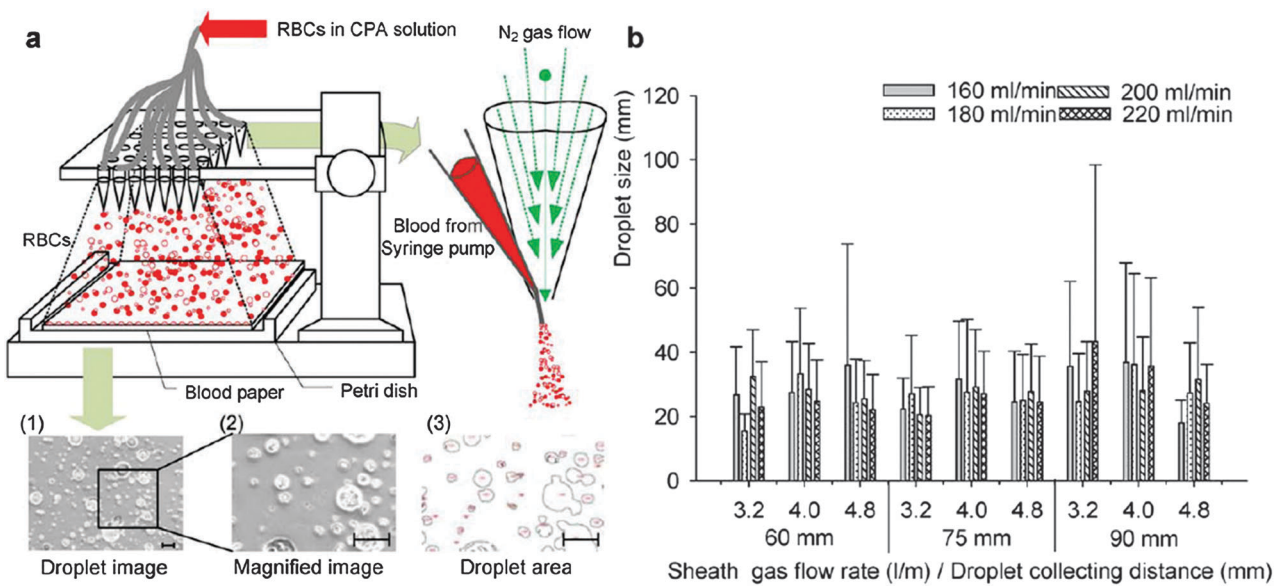

Fig. 11 A schematic of the blood cryopreservation platform. (a) Ejection and deposition of RBC encapsulating droplets on receiving paper (top) and droplet pictures (bottom). Scale bar is 500 μm. (b) Average size of ejected droplets is plotted for a range of sheath gas flow rates (3.2, 4.0, 4.8 L m^{-1}), blood flow rates (160, 180, 200, and 220 mL min^{-1}), and droplet collecting distances (60, 75, and 90 mm). *Reproduced with permission.*[224]

employing high CPA concentrations may require tedious manual steps during handling of cells between CPA loading and unloading solutions. Therefore, integration of nano-liter cell encapsulation technologies with vitrification can reduce manual steps, handling errors and operator variability.

Recently, a droplet ejection technology was developed to vitrify oocyte encapsulating nano-liter droplets.[226] This platform was utilized to vitrify and cryopreserve oocytes, which were encapsulated in nano-liter droplets at high-throughput.[226] During this vitrification process, morphologies of the mouse oocytes, their parthenogenetic development, and survival rates were compared to fresh oocytes cultured in the potassium simplex optimized medium (KSOM) right after retrieval. Similar survival rates were reported between the results of the droplet encapsulation method and the control group (*i.e.*, fresh oocytes after 24 h in culture). Morphologies of the oocytes and the rate of parthenogenetic activation were also comparable between the oocytes collected after vitrification/thawing and the fresh oocytes. Another important application of cryopreservation is blood banking.[224] Recently, RBC encapsulating nano-liter droplets (*e.g.*, radius < 100 μm) were vitrified at high throughput (Fig. 11).[224] A co-flow droplet ejection system (*i.e.*, nitrogen and RBC flow) was used to generate RBC encapsulating droplets. The effects of the experimental parameters: (1) the RBC flow rate (RBCs were loaded with CPA) (160 to 220 mL min^{-1}), (2) the nitrogen gas flow rate (3.2 to 4.8 L min^{-1}), and (3) the distance between the ejector tip and droplet receiving film (60 to 90 mm), were evaluated (Fig. 11).[224] To enable vitrification of RBCs with low CPA levels, nano-liter droplets were created in a continuous manner by adjusting the nitrogen gas flow rate. This approach minimized the possibility of negative osmotic and toxic effects by increasing cooling rates and using a low level of CPAs.[227,228] On the other hand, stem cells have been clinically essential due to their pluripotent potential and their role in regeneration of damaged tissues.[185] For stem cells, high CPA levels can cause uncontrolled differentiation and smaller viability.[219,220] Vitrification results in higher viabilities of stem cells compared to other methods including slow freezing.[229,240] Low CPA-level vitrification in nanoliter volumes has immense potential for stem cells compared to other methods in preserving their functionality.[219,220,229] Long-term biopreservation of cells in micro-scale volumes has a broad impact on multiple fields including tissue engineering, regenerative medicine, stem cells, blood banking, animal strain preservation (biodiversity protection), clinical sample storage, transplantation medicine and *in vitro* drug testing.

4. Conclusions and prospects

Manipulating cells in small volumes while maintaining viability and biological functionality has been a significant challenge for various applications in medicine. Advanced micro-scale manipulation technologies emerge at the convergence of multiple fields including basic sciences, engineering, and medicine. To address these challenges, several approaches have been developed based on magnetic, electrical, mechanical, acoustic, and fluidic principles. Among these approaches, bioprinting technologies are promising to achieve manipulation of cells and biological agents for applications in drug discovery, drug toxicity and efficacy testing, biopreservation and cancer research. On the other hand, development of microfluidic technologies has enabled miniaturization of traditional methods of manipulating, isolating, detecting and quantifying rare cells and molecules from bodily fluids. Due to simplicity, low cost and portability, microfluidic devices can be utilized widely across many disciplines to manipulate cells and biological agents in micro/nano-scale volumes. However, when a vast number of cells, different cell types and multiple scales are involved, challenges remain to be addressed in high-throughput applications of these technologies. Current challenges in micromanipulation of biological samples are the need for improved speed, flexibility, higher levels of automation, and contact-free operation. These challenges need to be addressed to make them widely available biological tools reducing manual operations without compromising accuracy and cost. To develop widely applicable methods that allow integration of various miniaturized devices on a single system, and parallel processing, a better understanding of microscale manipulation technologies is needed. Further, technologies are needed that have advantages including lower reagent and power consumption, portability, shorter reaction time, and lower cost to manipulate cells in micro-scale volumes. Future studies should also address the need for versatility, ease-of-use, scalability, and high-throughput utilization. These various challenges could be potentially addressed at the convergence of multiple fields.

Acknowledgements

We would like to acknowledge U54 EB015408, R21 HL112114, R01 AI093282, R01 AI081534, R21 AI087107, R21 HL095960, and R01 EB015776.

Notes and references

1 J. O. Kessler, *Nature*, 1985, **313**, 218–220.
2 N. Sundararajan, M. S. Pio, L. P. Lee and A. A. Berlin, *J. Microelectromech. Syst.*, 2004, **13**, 559–567.
3 G. B. Lee, B. H. Hwei and G. R. Huang, *J. Micromech. Microeng.*, 2001, **11**, 654–661.
4 Y. Du, E. Lo, S. Ali and A. Khademhosseini, *Proc. Natl. Acad. Sci. U. S. A.*, 2008, **105**, 9522–9527.
5 H. Lee, A. M. Purdon and R. M. Westervelt, *Appl. Phys. Lett.*, 2004, **85**, 1063–1065.
6 J. Yan, D. Skoko and J. F. Marko, *Phys. Rev. E: Stat. Nonlinear Soft Matter Phys.*, 2004, **70**, 011905.
7 F. Xu, C. A. Wu, V. Rengarajan, T. D. Finley, H. O. Keles, Y. Sung, B. Li, U. A. Gurkan and U. Demirci, *Adv. Mater.*, 2011, **23**, 4254–4260.
8 S. Tasoglu, D. Kavaz, U. A. Gurkan, S. Guven, P. Chen, R. Zheng and U. Demirci, *Adv. Mater.*, 2013, **25**, 1137–1143.

9 S. Srigunapalan, I. A. Eydelnant, C. A. Simmons and A. R. Wheeler, *Lab Chip*, 2012, **12**, 369–375.
10 D. Bogojevic, M. D. Chamberlain, I. Barbulovic-Nad and A. R. Wheeler, *Lab Chip*, 2012, **12**, 627–634.
11 M. P. Hughes, *Electrophoresis*, 2002, **23**, 2569–2582.
12 Y. K. Nahmias, B. Z. Gao and D. J. Odde, *Appl. Opt.*, 2004, **43**, 3999–4006.
13 Y. Nahmias, R. E. Schwartz, C. M. Verfaillie and D. J. Odde, *Biotechnol. Bioeng.*, 2005, **92**, 129–136.
14 D. G. Grier, *Nature*, 2003, **424**, 810–816.
15 M. P. MacDonald, G. C. Spalding and K. Dholakia, *Nature*, 2003, **426**, 421–424.
16 F. Xu, T. D. Finley, M. Turkaydin, Y. Sung, U. A. Gurkan, A. S. Yavuz, R. O. Guldiken and U. Demirci, *Biomaterials*, 2011, **32**, 7847–7855.
17 U. Demirci and G. Montesano, *Lab Chip*, 2007, **7**, 1139–1145.
18 R. P. Lanza, R. S. Langer and J. Vacanti, *Principles of tissue engineering*, Elsevier Academic Press, Amsterdam, Boston, 3rd edn, 2007.
19 U. A. Gurkan, S. Tasoglu, D. Kavaz, M. C. Demirel and U. Demirci, *Adv. Healthcare Mater.*, 2012, **1**, 149–158.
20 V. Mironov, R. P. Visconti, V. Kasyanov, G. Forgacs, C. J. Drake and R. R. Markwald, *Biomaterials*, 2009, **30**, 2164–2174.
21 S. Tasoglu and U. Demirci, *Trends Biotechnol.*, 2013, **31**, 10–19.
22 B. Guillotin, A. Souquet, S. Catros, M. Duocastella, B. Pippenger, S. Bellance, R. Bareille, M. Remy, L. Bordenave, J. Amedee and F. Guillemot, *Biomaterials*, 2010, **31**, 7250–7256.
23 F. Xu, J. H. Wu, S. Q. Wang, N. G. Durmus, U. A. Gurkan and U. Demirci, *Biofabrication*, 2011, **3**, 034101.
24 P. B. Malafaya, G. A. Silva and R. L. Reis, *Adv. Drug Delivery Rev.*, 2007, **59**, 207–233.
25 S. Nagrath, L. V. Sequist, S. Maheswaran, D. W. Bell, D. Irimia, L. Ulkus, M. R. Smith, E. L. Kwak, S. Digumarthy, A. Muzikansky, P. Ryan, U. J. Balis, R. G. Tompkins, D. A. Haber and M. Toner, *Nature*, 2007, **450**, 1235–1239.
26 S. Moon, U. A. Gurkan, J. Blander, W. W. Fawzi, S. Aboud, F. Mugusi, D. R. Kuritzkes and U. Demirci, *PLoS One*, 2011, **6**, e21409.
27 S. Moon, H. O. Keles, A. Ozcan, A. Khademhosseini, E. Haeggstrom, D. Kuritzkes and U. Demirci, *Biosens. Bioelectron.*, 2009, **24**, 3208–3214.
28 U. A. Gurkan, S. Moon, H. Geckil, F. Xu, S. Wang, T. J. Lu and U. Demirci, *Biotechnol. J.*, 2011, **6**, 138–149.
29 U. A. Gurkan, T. Anand, H. Tas, D. Elkan, A. Akay, H. O. Keles and U. Demirci, *Lab Chip*, 2011, **11**, 3979–3989.
30 U. A. Gurkan, S. Tasoglu, D. Akkaynak, O. Avci, S. Unluisler, S. Canikyan, N. MacCallum and U. Demirci, *Adv. Healthcare Mater.*, 2012, **1**, 661–668.
31 C. Yi, C.-W. Li, S. Ji and M. Yang, *Anal. Chim. Acta*, 2006, **560**, 1–23.
32 P. Y. Chiou, A. T. Ohta and M. C. Wu, *Nature*, 2005, **436**, 370–372.
33 J. R. Moffitt, Y. R. Chemla, S. B. Smith and C. Bustamante, *Annu. Rev. Biochem.*, 2008, **77**, 205–228.
34 L. R. Huang, E. C. Cox, R. H. Austin and J. C. Sturm, *Science*, 2004, **304**, 987–990.
35 A. Khademhosseini, J. Yeh, S. Jon, G. Eng, K. Y. Suh, J. A. Burdick and R. Langer, *Lab Chip*, 2004, **4**, 425–430.
36 N. Chronis and L. P. Lee, *J. Microelectromech. Syst.*, 2005, **14**, 857–863.
37 J. Yang, C. W. Li and M. S. Yang, *Lab Chip*, 2004, **4**, 53–59.
38 C. W. Li, C. N. Cheung, J. Yang, C. H. Tzang and M. S. Yang, *Analyst*, 2003, **128**, 1137–1142.
39 J. Voldman, *Annu. Rev. Biomed. Eng.*, 2006, **8**, 425–454.
40 H. Shafiee, M. Jahangir, F. Inci, S. Wang, R. B. M. Willenbrecht, F. F. Giguel, A. M. N. Tsibris, D. R. Kuritzkes and U. Demirci, *Small*, 2013, DOI: 10.1002/smll.201202195.
41 M. Goldberg, R. Langer and X. Q. Jia, *J. Biomater. Sci., Polym. Ed.*, 2007, **18**, 241–268.
42 U. A. Gurkan, Y. Fan, F. Xu, B. Erkmen, E. S. Urkac, G. Parlakgul, J. Bernstein, W. Xing, E. S. Boyden and U. Demirci, *Adv. Mater.*, 2013, **25**, 1192–1198.
43 M. D. Krebs, R. M. Erb, B. B. Yellen, B. Samanta, A. Bajaj, V. M. Rotello and E. Alsberg, *Nano Lett.*, 2009, **9**, 1812–1817.
44 W. R. Rodriguez, N. Christodoulides, P. N. Floriano, S. Graham, S. Mohanty, M. Dixon, M. Hsiang, T. Peter, S. Zavahir, I. Thior, D. Romanovicz, B. Bernard, A. P. Goodey, B. D. Walker and J. T. McDevitt, *PLoS Med.*, 2005, **2**, e182.
45 J. Voldman, M. L. Gray and M. A. Schmidt, *Annu. Rev. Biomed. Eng.*, 1999, **1**, 401–425.
46 G. M. Whitesides, E. Ostuni, S. Takayama, X. Jiang and D. E. Ingber, *Annu. Rev. Biomed. Eng.*, 2001, **3**, 335–373.
47 Y. S. Song, D. Adler, F. Xu, E. Kayaalp, A. Nureddin, R. M. Anchan, R. L. Maas and U. Demirci, *Proc. Natl. Acad. Sci. U. S. A.*, 2010, **107**, 4596–4600.
48 A. R. Kose, B. Fischer, L. Mao and H. Koser, *Proc. Natl. Acad. Sci. U. S. A.*, 2009, **106**, 21478–21483.
49 G. Frasca, F. Gazeau and C. Wilhelm, *Langmuir*, 2009, **25**, 2348–2354.
50 B. B. Yellen, O. Hovorka and G. Friedman, *Proc. Natl. Acad. Sci. U. S. A.*, 2005, **102**, 8860–8864.
51 C.-H. Chen, A. R. Abate, D. Lee, E. M. Terentjev and D. A. Weitz, *Adv. Mater.*, 2009, **21**, 3201–3204.
52 Q. Pankhurst, J. Connolly, S. K. Jones and J. Dobson, *J. Phys. D: Appl. Phys.*, 2003, **36**, R167–R181.
53 E. Alsberg, E. Feinstein, M. P. Joy, M. Prentiss and D. E. Ingber, *Tissue Eng.*, 2006, **12**, 3247–3256.
54 G. R. Souza, J. R. Molina, R. M. Raphael, M. G. Ozawa, D. J. Stark, C. S. Levin, L. F. Bronk, J. S. Ananta, J. Mandelin, M. M. Georgescu, J. A. Bankson, J. G. Gelovani, T. C. Killian, W. Arap and R. Pasqualini, *Nat. Nanotechnol.*, 2010, **5**, 291–296.
55 P. E. Le Renard, O. Jordan, A. Faes, A. Petri-Fink, H. Hofmann, D. Rufenacht, F. Bosman, F. Buchegger and E. Doelker, *Biomaterials*, 2010, **31**, 691–705.
56 Y. Li, G. Huang, X. Zhang, B. Li, Y. Chen, T. Lu, T. J. Lu and F. Xu, *Adv. Funct. Mater.*, 2013, **23**, 660–672.

57 C. B. Coleman, R. A. Gonzalez-Villalobos, P. L. Allen, K. Johanson, K. Guevorkian, J. M. Valles and T. G. Hammond, *Biotechnol. Bioeng.*, 2007, **98**, 854–863.
58 J. Dobson, *Nat. Nanotechnol.*, 2008, **3**, 139–143.
59 A. Ito, K. Ino, T. Kobayashi and H. Honda, *Biomaterials*, 2005, **26**, 6185–6193.
60 H. Akiyama, A. Ito, Y. Kawabe and M. Kamihira, *Biomed. Microdevices*, 2009, **11**, 713–721.
61 M. Okochi, S. Takano, Y. Isaji, T. Senga, M. Hamaguchi and H. Honda, *Lab Chip*, 2009, **9**, 3378–3384.
62 C. J. Meyer, F. J. Alenghat, P. Rim, J. H.-J. Fong, B. Fabry and D. E. Ingber, *Nat. Cell Biol.*, 2000, **2**, 666–668.
63 D. K. Hwang, D. Dendukuri and P. S. Doyle, *Lab Chip*, 2008, **8**, 1640–1647.
64 D. C. Pregibon, M. Toner and P. S. Doyle, *Langmuir*, 2006, **22**, 5122–5128.
65 K. P. Yuet, D. K. Hwang, R. Haghgooie and P. S. Doyle, *Langmuir*, 2010, **26**, 4281–4287.
66 K. W. Bong, S. C. Chapin and P. S. Doyle, *Langmuir*, 2010, **26**, 8008–8014.
67 N. Bowden, A. Terfort, J. Carbeck and G. M. Whitesides, *Science*, 1997, **276**, 233–235.
68 P. A. Kralchevsky, V. N. Paunov, N. D. Denkov, I. B. Ivanov and K. Nagayama, *J. Colloid Interface Sci.*, 1993, **155**, 420–437.
69 V. N. Paunov, P. A. Kralchevsky, N. D. Denkov and K. Nagayama, *J. Colloid Interface Sci.*, 1993, **157**, 100–112.
70 U. Demirci, *Rev. Sci. Instrum.*, 2005, **76**, 065103.
71 U. Demirci, *J. Microelectromech. Syst.*, 2006, **15**, 957–966.
72 U. Demirci, *Appl. Phys. Lett.*, 2006, **88**, 144104.
73 U. Demirci, A. S. Ergun, O. Oralkan, M. Karaman and B. T. Khuri-Yakub, *IEEE Trans. Ultrason. Ferroelectr. Freq. Control*, 2004, **51**, 887–895.
74 U. Demirci and A. Ozcan, *Electron. Lett.*, 2005, **41**, 1219–1220.
75 U. Demirci and M. Toner, *Appl. Phys. Lett.*, 2006, **88**, 053117.
76 U. Demirci, G. G. Yaralioglu, E. Haeggstrom and B. T. Khuri-Yakub, *IEEE Trans. Semicond. Manuf.*, 2005, **18**, 709–715.
77 U. Demirci, G. G. Yaralioglu, E. Haeggstrom, G. Percin, S. Ergun and B. T. Khuri-Yakub, *IEEE Trans. Semicond. Manuf.*, 2004, **17**, 517–524.
78 U. Demirci and G. Montesano, *Lab Chip*, 2007, **7**, 1428–1433.
79 Y. Fang, J. P. Frampton, S. Raghavan, R. Sabahi-Kaviani, G. Luker, C. X. Deng and S. Takayama, *Tissue Eng., Part C*, 2012, **18**, 647–657.
80 T. Boland, T. Xu, B. Damon and X. Cui, *Biotechnol. J.*, 2006, **1**, 910–917.
81 M. Nakamura, A. Kobayashi, F. Takagi, A. Watanabe, Y. Hiruma, K. Ohuchi, Y. Iwasaki, M. Horie, I. Morita and S. Takatani, *Tissue Eng.*, 2005, **11**, 1658–1666.
82 S. Moon, S. K. Hasan, Y. S. Song, F. Xu, H. O. Keles, F. Manzur, S. Mikkilineni, J. W. Hong, J. Nagatomi, E. Haeggstrom, A. Khademhosseini and U. Demirci, *Tissue Eng., Part C*, 2010, **16**, 157–166.
83 S. Moon, Y. G. Kim, L. Dong, M. Lombardi, E. Haeggstrom, R. V. Jensen, L. L. Hsiao and U. Demirci, *PLoS One*, 2011, **6**, e17455.
84 D. J. Odde and M. J. Renn, *Trends Biotechnol.*, 1999, **17**, 385–389.
85 S. A. Elrod, B. Hadimioglu, B. T. Khuriyakub, E. G. Rawson, E. Richley, C. F. Quate, N. N. Mansour and T. S. Lundgren, *J. Appl. Phys.*, 1989, **65**, 3441–3447.
86 S. Moon, E. Ceyhan, U. A. Gurkan and U. Demirci, *PLoS One*, 2011, **6**, e21580.
87 E. Ceyhan, F. Xu, U. A. Gurkan, A. E. Emre, E. S. Turali, R. El Assal, A. Acikgenc, C. M. Wu and U. Demirci, *Lab Chip*, 2012, **12**, 4884–4893.
88 W. Wang, Y. Huang, M. Grujicic and D. B. Chrisey, *J. Manuf. Sci. Eng.*, 2008, **130**, 021012.
89 S. Tasoglu, G. Kaynak, A. J. Szeri, U. Demirci and M. Muradoglu, *Phys. Fluids*, 2010, **22**, 082103.
90 M. Muradoglu and S. Tasoglu, *Comput. Fluids.*, 2010, **39**, 615–625.
91 M. Muradoglu and S. Tasoglu, *ASME*, 2009, **2009**, 1095–1106.
92 H. Takamatsu and B. Rubinsky, *Cryobiology*, 1999, **39**, 243–251.
93 S. Wang, F. Inci, G. De Libero, A. Singhal and U. Demirci, *Biotechnol. Adv.*, 2013, DOI: 10.1016/j.biotechadv.2013.01.006.
94 S. Wang, F. Xu and U. Demirci, *Biotechnol. Adv.*, 2010, **28**, 770–781.
95 World Health Organization, 2009, Accessed on February 4, 2013.
96 B. R. Zetter, *Annu. Rev. Med.*, 1998, **49**, 407–424.
97 M. Cristofanilli, G. T. Budd, M. J. Ellis, A. Stopeck, J. Matera, M. C. Miller, J. M. Reuben, G. V. Doyle, W. J. Allard, L. W. M. M. Terstappen and D. F. Hayes, *New Engl. J. Med.*, 2004, **351**, 781–791.
98 S. Maheswaran, L. V. Sequist, S. Nagrath, L. Ulkus, B. Brannigan, C. V. Collura, E. Inserra, S. Diederichs, A. J. Iafrate, D. W. Bell, S. Digumarthy, A. Muzikansky, D. Irimia, J. Settleman, R. G. Tompkins, T. J. Lynch, M. Toner and D. A. Haber, *New Engl. J. Med.*, 2008, **359**, 366–377.
99 S. L. Stott, R. J. Lee, S. Nagrath, M. Yu, D. T. Miyamoto, L. Ulkus, E. J. Inserra, M. Ulman, S. Springer, Z. Nakamura, A. L. Moore, D. I. Tsukrov, M. E. Kempner, D. M. Dahl, C. L. Wu, A. J. Iafrate, M. R. Smith, R. G. Tompkins, L. V. Sequist, M. Toner, D. A. Haber and S. Maheswaran, *Sci. Transl. Med.*, 2010, **2**, 25ra23.
100 S. E. Cross, Y. S. Jin, J. Rao and J. K. Gimzewski, *Nat. Nanotechnol.*, 2007, **2**, 780–783.
101 R. de la Rica, S. Thompson, A. Baldi, C. Fernandez-Sanchez, C. M. Drain and H. Matsui, *Anal. Chem.*, 2009, **81**, 10167–10171.
102 A. A. Adams, P. I. Okagbare, J. Feng, M. L. Hupert, D. Patterson, J. Gottert, R. L. McCarley, D. Nikitopoulos, M. C. Murphy and S. A. Soper, *J. Am. Chem. Soc.*, 2008, **130**, 8633–8641.
103 H. Zhang, A. Berezov, Q. Wang, G. Zhang, J. Drebin, R. Murali and M. I. Greene, *J. Clin. Invest.*, 2007, **117**, 2051–2058.

104 Q. Abdool Karim, S. S. Abdool Karim, J. A. Frohlich, A. C. Grobler, C. Baxter, L. E. Mansoor, A. B. M. Kharsany, S. Sibeko, K. P. Mlisana, Z. Omar, T. N. Gengiah, S. Maarschalk, N. Arulappan, M. Mlotshwa, L. Morris, D. Taylor and On behalf of the CAPRISA 004 Trial Group, *Science*, 2010, **329**, 1168–1174.
105 S. Tasoglu, S. C. Park, J. J. Peters, D. F. Katz and A. J. Szeri, *J. Non-Newtonian Fluid Mech.*, 2011, **166**, 1116–1122.
106 S. Tasoglu, J. J. Peters, S. C. Park, S. Verguet, D. F. Katz and A. J. Szeri, *Phys. Fluids*, 2011, **23**, 093101.
107 S. Tasoglu, A. J. Szeri and D. F. Katz, *Biophys. J.*, 2011, **100**, 489.
108 S. Tasoglu, D. F. Katz and A. J. Szeri, *J. Non-Newtonian Fluid Mech.*, 2012, **187**, 36–42.
109 A. J. Szeri, S. C. Park, S. Tasoglu, S. Verguet, A. Gorham, Y. Gao and D. F. Katz, *Biophys. J.*, 2010, **98**, 604.
110 S. Tasoglu, L. C. Rohan, D. F. Katz and A. J. Szeri, *Phys. Fluids*, 2013, **25**, 031901.
111 UNAIDS, Report on the global AIDS epidemic. Available at http://data.unaids.org/pub/GlobalReport/2008/JC1510_2008 GlobalReport_en.zip. Accessed: January 2027th 2013.
112 A. Ozcan and U. Demirci, *Lab Chip*, 2008, **8**, 98–106.
113 J. V. Jokerst, P. N. Floriano, N. Christodoulides, G. W. Simmons and J. T. McDevitt, *Lab Chip*, 2008, **8**, 2079–2090.
114 M. A. Alyassin, S. Moon, H. O. Keles, F. Manzur, R. L. Lin, E. Haeggstrom, D. R. Kuritzkes and U. Demirci, *Lab Chip*, 2009, **9**, 3364–3369.
115 X. H. Zhang, I. Khimji, U. A. Gurkan, H. Safaee, P. N. Catalano, H. O. Keles, E. Kayaalp and U. Demirci, *Lab Chip*, 2011, **11**, 2535–2540.
116 X. Cheng, Y.-s. Liu, D. Irimia, U. Demirci, L. Yang, L. Zamir, W. R. Rodriguez, M. Toner and R. Bashir, *Lab Chip*, 2007, **7**, 746–755.
117 X. Cheng, D. Irimia, M. Dixon, J. C. Ziperstein, U. Demirci, L. Zamir, R. G. Tompkins, M. Toner and W. R. Rodriguez, *J. Acquired Immune Defic. Syndr.*, 2007, **45**, 257–261.
118 X. H. Cheng, A. Gupta, C. C. Chen, R. G. Tompkins, W. Rodriguez and M. Toner, *Lab Chip*, 2009, **9**, 1357–1364.
119 S. Wang, F. Inci, T. L. Chaunzwa, A. Ramanujam, A. Vasudevan, S. Subramanian, A. Chi Fai Ip, B. Sridharan, U. A. Gurkan and U. Demirci, *Int. J. Nanomed.*, 2012, **7**, 2591–2600.
120 M. W. Sanderson, S. Sreerama and T. G. Nagaraja, *Curr. Microbiol.*, 2007, **55**, 158–161.
121 S. T. Fan, C. H. Teoh-Chan and K. F. Lau, *Eur. J. Clin. Microbiol. Infect. Dis.*, 1989, **8**, 142–144.
122 N. Quilici, G. Audibert, M. C. Conroy, P. E. Bollaert, F. Guillemin, P. Welfringer, J. Garric, M. Weber and M. C. Laxenaire, *Clin. Infect. Dis.*, 1997, **25**, 1066–1070.
123 World Health Organization, 2010, http://www.who.int/hiv/pub/paediatric/diagnosis/en/index.html. Accessed: January 27th 2013.
124 Y. G. Kim, S. Moon, D. R. Kuritzkes and U. Demirci, *Biosens. Bioelectron.*, 2009, **25**, 253–258.
125 S. Wang, M. Esfahani, U. A. Gurkan, F. Inci, D. R. Kuritzkes and U. Demirci, *Lab Chip*, 2012, **12**, 1508–1515.
126 N. Tang, S. Huang, J. Salituro, W. B. Mak, G. Cloherty, J. Johanson, Y. H. Li, G. Schneider, J. Robinson, J. Hackett Jr., P. Swanson and K. Abravaya, *J. Virol. Methods*, 2007, **146**, 236–245.
127 B. S. Taylor, M. E. Sobieszczyk, F. E. McCutchan and S. M. Hammer, *New Engl. J. Med.*, 2008, **358**, 1590–1602.
128 S. Wang, D. Sarenac, M. Chen, S. Huang, F. Giguel, D. Kuritzkes and U. Demirci, *Int. J. Nanomed.*, 2012, **7**, 5019–5028.
129 M. Yang, S. Sun, Y. Kostov and A. Rasooly, *Lab Chip*, 2010, **10**, 1011–1017.
130 S. Wang, X. Zhao, I. Khimji, R. Akbas, W. Qiu, D. Edwards, D. W. Cramer, B. Ye and U. Demirci, *Lab Chip*, 2011, **11**, 3411–3418.
131 D. L. Clarke-Pearson, *New Engl. J. Med.*, 2009, **361**, 170–177.
132 Centers for disease control and prevention, available at http://www.cdc.gov/reproductivehealth/infertility/. Accessed: January 27th 2013.
133 J. Saragusty and A. Arav, *Reproduction*, 2011, **141**, 1–19.
134 B. S. Cho, T. G. Schuster, X. Y. Zhu, D. Chang, G. D. Smith and S. Takayama, *Anal. Chem.*, 2003, **75**, 1671–1675.
135 T. Hyakutake, Y. Hashimoto, S. Yanase, K. Matsuura and K. Naruse, *Biomed. Microdevices*, 2009, **11**, 25–33.
136 R. Ma, L. Xie, C. Han, K. Su, T. Qiu, L. Wang, G. Huang, W. Xing, J. Qiao, J. Wang and J. Cheng, *Anal. Chem.*, 2011, **83**, 2964–2970.
137 M. D. Lopez-Garcia, R. L. Monson, K. Haubert, M. B. Wheeler and D. J. Beebe, *Biomed. Microdevices*, 2008, **10**, 709–718.
138 T. G. Schuster, B. Cho, L. M. Keller, S. Takayama and G. D. Smith, *Reprod. BioMed. Online*, 2003, **7**, 75–81.
139 L. Xie, R. Ma, C. Han, K. Su, Q. Zhang, T. Qiu, L. Wang, G. Huang, J. Qiao, J. Wang and J. Cheng, *Clin. Chem.*, 2010, **56**, 1270–1278.
140 H. Winet, G. S. Bernstein and J. Head, *J. Reprod. Fertil.*, 1984, **70**, 511–523.
141 S. Tasoglu, H. Safaee, X. Zhang, J. L. Kingsley, P. N. Catalano, U. A. Gurkan, A. Nureddin, E. Kayaalp, R. M. Anchan, L. Maas, E. Tüzel and U. Demirci, *Small*, 2013, DOI: 10.1002/smll.201300020.
142 K. T. Kotz, W. Xiao, C. Miller-Graziano, W.-J. Qian, A. Russom, E. A. Warner, L. L. Moldawer, A. De, P. E. Bankey, B. O. Petritis, D. G. Camp, A. E. Rosenbach, J. Goverman, S. P. Fagan, B. H. Brownstein, D. Irimia, W. Xu, J. Wilhelmy, M. N. Mindrinos, R. D. Smith, R. W. Davis, R. G. Tompkins and M. Toner, *Nat. Med.*, 2010, **16**, 1042–1047.
143 A. Salehi-Reyhani, J. Kaplinsky, E. Burgin, M. Novakova, A. J. Demello, R. H. Templer, P. Parker, M. A. A. Neil, O. Ces, P. French, K. R. Willison and D. Klug, *Lab Chip*, 2011, **11**, 1256–1261.
144 B. K. McKenna, A. A. Selim, F. R. Bringhurst and D. J. Ehrlich, *Lab Chip*, 2009, **9**, 305–310.
145 Q. Ramadan, V. Samper, D. Poenar, Z. Liang, C. Yu and T. M. Lim, *Sens. Actuators, B*, 2006, **113**, 944–955.
146 M. Hosokawa, A. Arakaki, M. Takahashi, T. Mori, H. Takeyama and T. Matsunaga, *Anal. Chem.*, 2009, **81**, 5308–5313.

147 H. W. Wu, C. C. Lin and G. B. Lee, *Biomicrofluidics*, 2011, **5**, 26.
148 Y. Xu, J. A. Phillips, J. L. Yan, Q. G. Li, Z. H. Fan and W. H. Tan, *Anal. Chem.*, 2009, **81**, 7436–7442.
149 K. Wang, B. Cometti and D. Pappas, *Anal. Chim. Acta*, 2007, **601**, 1–9.
150 Y. Sung-Yi, H. Suz-Kai, H. Yung-Ching, C. Chen-Min, L. Teh-Lu and L. Gwo-Bin, *Meas. Sci. Technol.*, 2006, **17**, 2001.
151 A. Y. Fu, H.-P. Chou, C. Spence, F. H. Arnold and S. R. Quake, *Anal. Chem.*, 2002, **74**, 2451–2457.
152 X. Zhang, P. Jones and S. J. Haswell, *Chem. Eng. J.*, 2008, **135**, S82–S88.
153 S. P. Wankhede, Z. Du, J. M. Berg, M. W. Vaughn, T. Dallas, K. H. Cheng and L. Gollahon, *Biotechnol. Prog.*, 2006, **22**, 1426–1433.
154 B. D. Plouffe, M. A. Brown, R. K. Iyer, M. Radisic and S. K. Murthy, *Lab Chip*, 2009, **9**, 1507–1510.
155 K. Jung, G. Hampel, M. Scholz and W. Henke, *Cell. Physiol. Biochem.*, 1995, **5**, 353–360.
156 N. Fujioka, Y. Morimoto, K. Takeuchi, M. Yoshioka and M. Kikuchi, *Appl. Spectrosc.*, 2003, **57**, 241–243.
157 A. Hatch, G. Hansmann and S. K. Murthy, *Langmuir*, 2011, **27**, 4257–4264.
158 D. Suárez-González, K. Barnhart, E. Saito, R. Vanderby, S. J. Hollister and W. L. Murphy, *J. Biomed. Mater. Res., Part A*, 2010, **95**, 222–234.
159 H. Kanazawa, K. Yamamoto, Y. Kashiwase, Y. Matsushima, N. Takai, A. Kikuchi, Y. Sakurai and T. Okano, *J. Pharm. Biomed. Anal.*, 1997, **15**, 1545–1550.
160 D. L. Huber, R. P. Manginell, M. A. Samara, B. I. Kim and B. C. Bunker, *Science*, 2003, **301**, 352–354.
161 N. Lion, T. C. Rohner, L. Dayon, I. L. Arnaud, E. Damoc, N. Youhnovski, Z.-Y. Wu, C. Roussel, J. Josserand, H. Jensen, J. S. Rossier, M. Przybylski and H. H. Girault, *Electrophoresis*, 2003, **24**, 3533–3562.
162 T. M. Tarasow, L. Penny, A. Patwardhan, S. Hamren, M. P. McKenna and M. S. Urdea, *Bioanalysis*, 2011, **3**, 2233–2251.
163 R. Langer and J. P. Vacanti, *Science*, 1993, **260**, 920–926.
164 A. Khademhosseini, R. Langer, J. Borenstein and J. P. Vacanti, *Proc. Natl. Acad. Sci. U. S. A.*, 2006, **103**, 2480–2487.
165 G. T. Kose, H. Kenar, N. Hasirci and V. Hasirci, *Biomaterials*, 2003, **24**, 1949–1958.
166 R. E. Unger, A. Sartoris, K. Peters, A. Motta, C. Migliaresi, M. Kunkel, U. Bulnheim, J. Rychly and C. J. Kirkpatrick, *Biomaterials*, 2007, **28**, 3965–3976.
167 A. J. Salgado, O. P. Coutinho and R. L. Reis, *Macromol. Biosci.*, 2004, **4**, 743–765.
168 U. A. Gurkan, X. G. Cheng, V. Kishore, J. A. Uquillas and O. Akkus, *J. Biomed. Mater. Res., Part A*, 2010, **94**, 1070–1079.
169 U. A. Gurkan, J. Gargac and O. Akkus, *Tissue Eng., Part A*, 2010, **16**, 2295–2306.
170 U. A. Gurkan, V. Kishore, K. W. Condon, T. M. Bellido and O. Akkus, *Calcif. Tissue Int.*, 2011, **88**, 388–401.
171 U. A. Gurkan, A. Krueger and O. Akkus, *Tissue Eng., Part A*, 2011, **17**, 417–428.
172 E. M. Christenson, K. S. Anseth, L. van den Beucken, C. K. Chan, B. Ercan, J. A. Jansen, C. T. Laurencin, W. J. Li, R. Murugan, L. S. Nair, S. Ramakrishna, R. S. Tuan, T. J. Webster and A. G. Mikos, *J. Orthop. Res.*, 2007, **25**, 11–22.
173 T. J. Cho, L. C. Gerstenfeld and T. A. Einhorn, *J. Bone Miner. Res.*, 2002, **17**, 513–520.
174 A. X. Le, T. Miclau, D. Hu and J. A. Helms, *J. Orthop. Res.*, 2001, **19**, 78–84.
175 K. Tatsuyama, Y. Maezawa, H. Baba, Y. Imamura and M. Fukuda, *Eur. J. Histochem.*, 2000, **44**, 269–278.
176 A. Muraglia, I. Martin, R. Cancedda and R. Quarto, *Bone*, 1998, **22**, 131s–134s.
177 T. Histing, P. Garcia, R. Matthys, M. Leidinger, J. H. Holstein, A. Kristen, T. Pohlemann and M. D. Menger, *J. Orthop. Res.*, 2010, **28**, 397–402.
178 Z. Thompson, T. Miclau, D. Hu and J. A. Helms, *J. Orthop. Res.*, 2002, **20**, 1091–1098.
179 M. Radisic and G. Vunjak-Novakovic, *J. Serb. Chem. Soc.*, 2005, **70**, 541–556.
180 J. T. Borenstein, H. Terai, K. R. King, E. J. Weinberg, M. R. Kaazempur-Mofrad and J. P. Vacanti, *Biomed. Microdevices*, 2002, **4**, 167–175.
181 N. Bursac, K. K. Parker, S. Iravanian and L. Tung, *Circ. Res.*, 2002, **91**, e45–e54.
182 C. Fidkowski, M. R. Kaazempur-Mofrad, J. Borenstein, J. P. Vacanti, R. Langer and Y. Wang, *Tissue Eng.*, 2005, **11**, 302–309.
183 R. K. Li, T. M. Yau, R. D. Weisel, D. A. Mickle, T. Sakai, A. Choi and Z. Q. Jia, *J. Thorac. Cardiovasc. Surg.*, 2000, **119**, 368–375.
184 K. S. Masters, D. N. Shah, L. A. Leinwand and K. S. Anseth, *Biomaterials*, 2005, **26**, 2517–2525.
185 H. Geckil, F. Xu, X. H. Zhang, S. Moon and U. Demirci, *Nanomedicine*, 2010, **5**, 469–484.
186 K. Y. Lee and D. J. Money, *Chem. Rev.*, 2001, **101**, 1869.
187 L. G. Griffith and M. A. Swartz, *Nat. Rev.: Mol. Cell Biol.*, 2006, **7**, 211–224.
188 C. Fischbach, R. Chen, T. Matsumoto, T. Schmelzle, J. S. Brugge, P. J. Polverini and D. J. Mooney, *Nat. Methods*, 2007, **4**, 855–860.
189 M. W. Tibbitt and K. S. Anseth, *Biotechnol. Bioeng.*, 2009, **103**, 655–663.
190 S. Yang, K. F. Leong, Z. Du and C. K. Chua, *Tissue Eng.*, 2002, **8**, 1–11.
191 J. A. Barron, P. Wu, H. D. Ladouceur and B. R. Ringeisen, *Biomed. Microdevices*, 2004, **6**, 139–147.
192 T. Xu, C. A. Gregory, P. Molnar, X. Cui, S. Jalota, S. B. Bhaduri and T. Boland, *Biomaterials*, 2006, **27**, 3580–3588.
193 R. R. Sinden, *Nature*, 2001, **411**, 757–758.
194 C. A. Ross and M. A. Poirier, *Nat. Med.*, 2004, **10**(Suppl.), S10–S17.
195 K. J. Barnham, C. L. Masters and A. I. Bush, *Nat. Rev. Drug Discovery*, 2004, **3**, 205–214.

196 E. Wong and A. M. Cuervo, *Nat. Neurosci.*, 2010, **13**, 805–811.
197 E. J. Bradbury and S. B. McMahon, *Nat. Rev. Neurosci.*, 2006, **7**, 644–653.
198 S. Woerly, O. Awosika, P. Zhao, C. Agbo, F. Gomez-Pinilla, J. de Vellis and A. Espinosa-Jeffrey, *Neurochem. Res.*, 2005, **30**, 721–735.
199 E. Lavik, *Neural Tissue Engineering*, Springer, New York, 2011.
200 K. Musick, D. Khatami and B. C. Wheeler, *Lab Chip*, 2009, **9**, 2036–2042.
201 J. Silver and J. H. Miller, *Nat. Rev. Neurosci.*, 2004, **5**, 146–156.
202 D. H. Kim, J. Viventi, J. J. Amsden, J. L. Xiao, L. Vigeland, Y. S. Kim, J. A. Blanco, B. Panilaitis, E. S. Frechette, D. Contreras, D. L. Kaplan, F. G. Omenetto, Y. G. Huang, K. C. Hwang, M. R. Zakin, B. Litt and J. A. Rogers, *Nat. Mater.*, 2010, **9**, 511–517.
203 R. G. Wylie, S. Ahsan, Y. Aizawa, K. L. Maxwell, C. M. Morshead and M. S. Shoichet, *Nat. Mater.*, 2011, **10**, 799–806.
204 S. N. Bailey, D. M. Sabatini and B. R. Stockwell, *Proc. Natl. Acad. Sci. U. S. A.*, 2004, **101**, 16144–16149.
205 M. Y. Lee, C. B. Park, J. S. Dordick and D. S. Clark, *Proc. Natl. Acad. Sci. U. S. A.*, 2005, **102**, 983–987.
206 S. Upadhyaya and P. R. Selvaganapathy, *Lab Chip*, 2010, **10**, 341–348.
207 D. N. Gosalia and S. L. Diamond, *Proc. Natl. Acad. Sci. U. S. A.*, 2003, **100**, 8721–8726.
208 H. Ma, K. Y. Horiuchi, Y. Wang, S. A. Kucharewicz and S. L. Diamond, *Assay Drug Dev. Technol.*, 2005, **3**, 177–187.
209 V. Starkuviene, R. Pepperkok and H. Erfle, *Expert Rev. Proteomics*, 2007, **4**, 479–489.
210 D. S. Chen and M. M. Davis, *Curr. Opin. Chem. Biol*, 2006, **10**, 28–34.
211 M. L. Yarmush and K. R. King, *Annu. Rev. Biomed. Eng.*, 2009, **11**, 235–257.
212 X. Gidrol, B. Fouque, L. Ghenim, V. Haguet, N. Picollet-D'hahan and B. Schaack, *Curr. Opin. Pharmacol.*, 2009, **9**, 664–668.
213 S. Guven and U. Demirci, *Nanomedicine*, 2012, **7**, 1787–1789.
214 P. Windrum, T. C. Morris, M. B. Drake, D. Niederwieser and T. Ruutu, *Bone Marrow Transplant.*, 2005, **36**, 601–603.
215 P. Desrosiers, C. Légaré, P. Leclerc and R. Sullivan, *Fertil. Steril.*, 2006, **85**, 1744–1752.
216 R. Fabbri, E. Porcu, T. Marsella, G. Rocchetta, S. Venturoli and C. Flamigni, *Hum. Reprod.*, 2001, **16**, 411–416.
217 F. Xu, S. J. Moon, A. E. Emre, E. S. Turali, Y. S. Song, S. A. Hacking, J. Nagatomi and U. Demirci, *Biofabrication*, 2010, **2**, 014105.
218 Y. S. Song, S. Moon, L. Hulli, S. K. Hasan, E. Kayaalp and U. Demirci, *Lab Chip*, 2009, **9**, 1874–1881.
219 L. Ji, J. J. de Pablo and S. P. Palecek, *Biotechnol. Bioeng.*, 2004, **88**, 299–312.
220 B. Hegner, M. Weber, D. Dragun and E. Schulze-Lohoff, *J. Hypertens.*, 2005, **23**, 1191–1202.
221 J. J. Stachecki and J. Cohen, *Reprod. BioMed. Online*, 2004, **9**, 152–163.
222 M. Ludwig, S. Al-Hasani, R. Felberbaum and K. Diedrich, *Hum. Reprod.*, 1999, **14**, 162–185.
223 U. Demirci, A. Khademhosseini, R. Langer and J. Blander, *Microfluidic Technologies for Human Health*, World Scientific Publishing Company, 2012.
224 J. Samot, S. Moon, L. Shao, X. Zhang, F. Xu, Y. Song, H. O. Keles, L. Matloff, J. Markel and U. Demirci, *PLoS One*, 2011, **6**, e17530.
225 B. J. Fuller, *CryoLetters*, 2004, **25**, 375–388.
226 X. Zhang, I. Khimji, L. Shao, H. Safaee, K. Desai, H. O. Keles, U. A. Gurkan, E. Kayaalp, A. Nureddin, R. M. Anchan, R. L. Maas and U. Demirci, *Nanomedicine*, 2012, **7**, 553–564.
227 H. T. Meryman and M. Hornblower, *Transfusion*, 1972, **12**, 145–156.
228 J. L. Tullis, M. M. Ketchel, H. M. Pyle, R. B. Pennell, J. G. Gibson 2nd, R. J. Tinch and S. G. Driscoll, *JAMA, J. Am. Med. Assoc.*, 1958, **168**, 399–404.
229 F. C. K. Tan, K. H. Lee, S. S. Gouk, R. Magalhaes, A. Poonepalli, M. P. Hande, G. S. Dawe and L. L. Kuleshova, *CryoLetters*, 2007, **28**, 445–460.
230 M. Berger, J. Castelino, R. Huang, M. Shah and R. H. Austin, *Electrophoresis*, 2001, **22**, 3883–3892.
231 V. I. Furdui and D. J. Harrison, *Lab Chip*, 2004, **4**, 614–618.
232 D. W. Inglis, R. Riehn, R. H. Austin and J. C. Sturm, *Appl. Phys. Lett.*, 2004, **85**, 5093–5095.
233 F. Xu, F. Inci, O. Mullick, U. A. Gurkan, Y. Sung, D. Kavaz, B. Li, E. B. Denkbas and U. Demirci, *ACS Nano*, 2012, **6**, 6640–6649.
234 S. E. Chung, W. Park, S. Shin, S. A. Lee and S. Kwon, *Nat. Mater.*, 2008, **7**, 581–587.
235 W. Park, H. Lee, H. Park and S. Kwon, *Lab Chip*, 2009, **9**, 2169–2175.
236 S. E. Chung, Y. Jung and S. Kwon, *Small*, 2011, **7**, 796–803.
237 K. Sekeroglu, U. A. Gurkan, U. Demirci and M. C. Demirel, *Appl. Phys. Lett.*, 2011, **99**, 63703–637033.
238 *Wettability*, ed. S. F. Kistler, Dekker, New York, 1993.
239 R. Won, *Nat. Photonics*, 2011, **5**, 512.
240 X. Zhang, P. N. Catalono, U. A. Gurkan, P. I. Khimji and U. Demirci, *Nanomedicine*, 2011, **6**, 1115–1129.